

EoS in Astrophysics, Argonne, 26. 08. 08

Mott Dissociation of Bound States in Nuclear Matter

Gerd Röpke, Rostock

ESF RNP CompStar

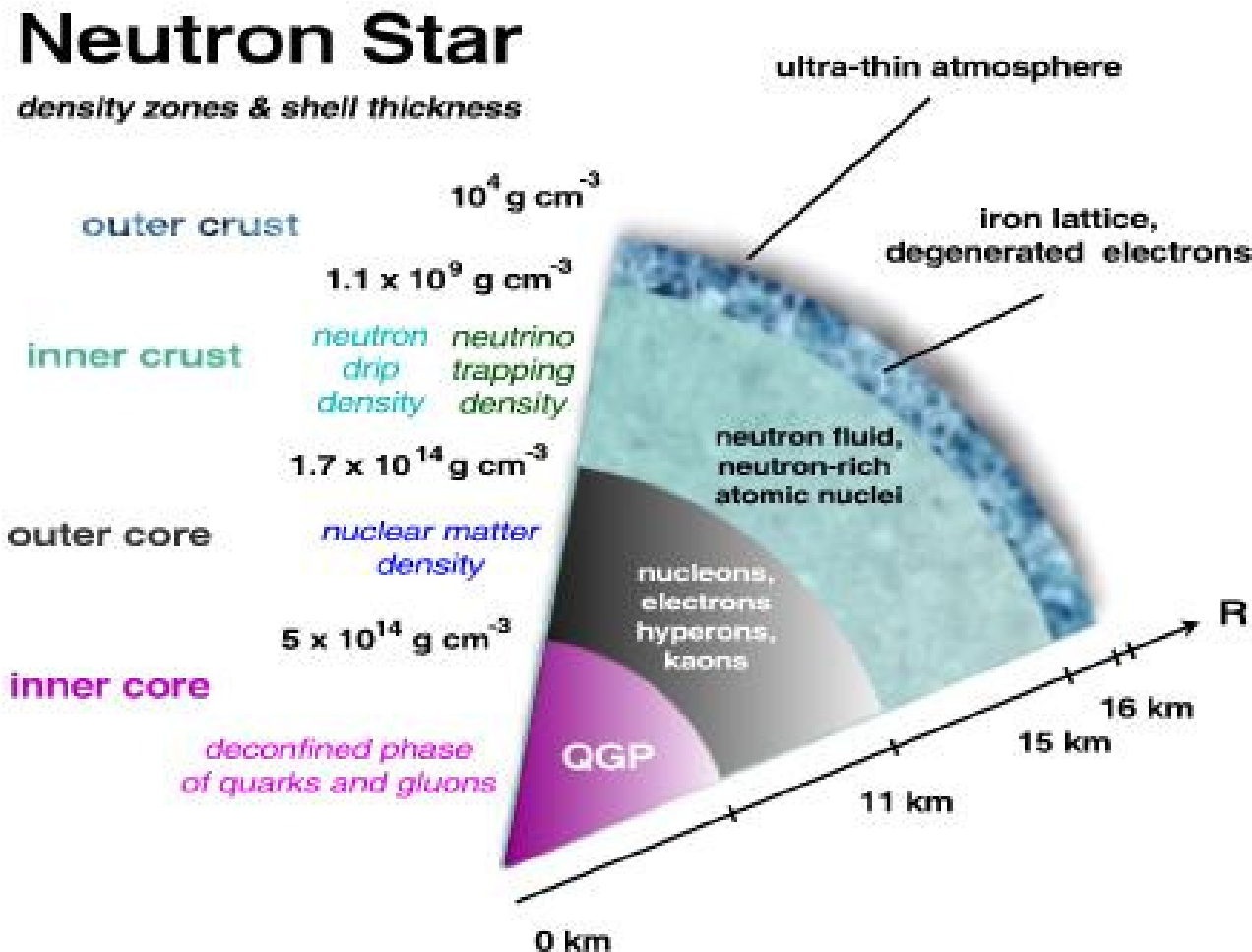


Supernova

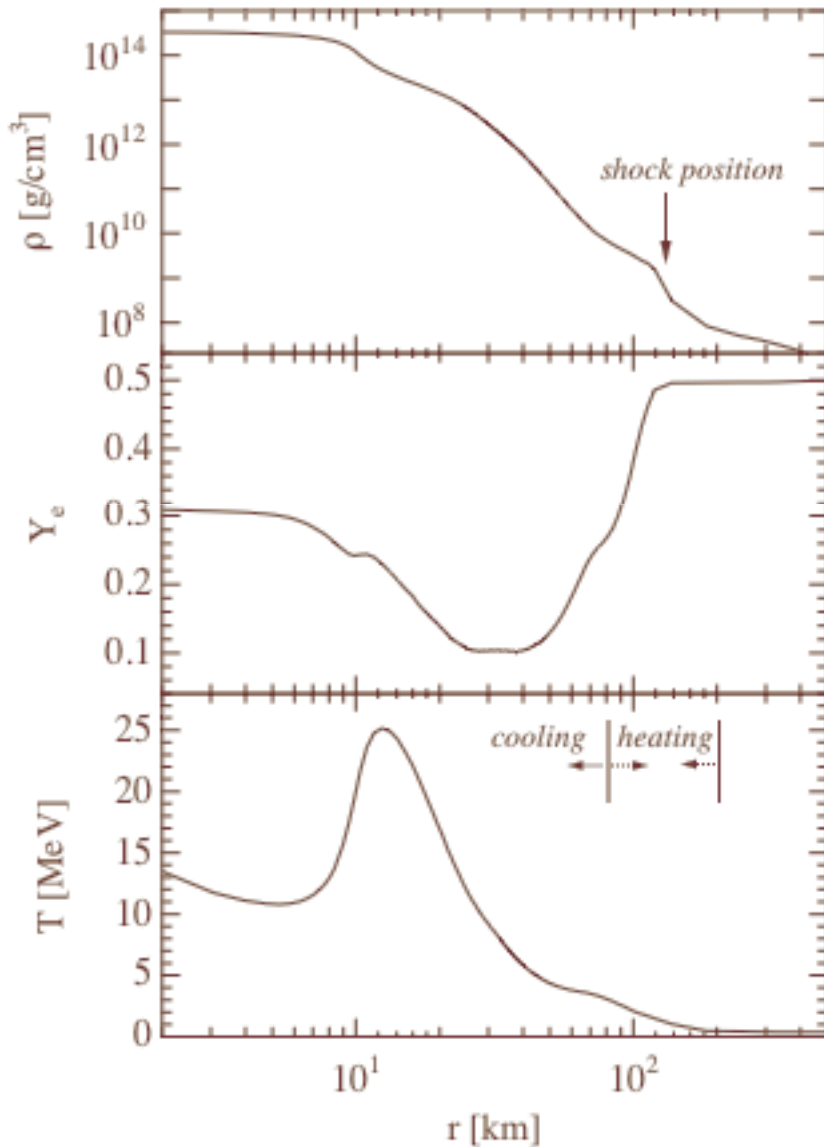
Crab nebula, 1054 China, PSR 0531+21



Structure of a Neutron star



Core-collapse supernovae



Density,
electron fraction, and
temperature profile
of a 15 solar mass supernova
at 150 ms after core bounce
as function of the radius.

Influence of cluster formation
on neutrino emission
in the cooling region and
on neutrino absorption
in the heating region ?

K.Sumiyoshi et al.,
Astrophys.J. **629**, 922 (2005)

Supernova collapse: spherically symmetric simulations

QuickTime™ and a
TIFF (LZW) decompressor
are needed to see this picture.

A. Arcones et al.
Neutrino driven winds,
Talk 25. 2. 08 Ladek;
PRC 78, 015806 (08)

Parameter range: Explosion

QuickTime™ and a
TIFF (LZW) decompressor
are needed to see this picture.

T. Fischer, On the possible fate of massive progenitor stars, Talk 25.2.08 Ladek

Problems:

- Warm Dilute Matter: Nuclear matter at subsaturation densities (T , n_p , n_n):
Temperature $T \leq 16$ MeV = E_s/A , baryon density $n_B \leq 0.17$ fm $^{-3}$ = n_s , asymmetry
- Formation of clusters (nuclei in matter):
 $A = 1,2,3,4$: free neutrons, free protons, deuterons (2H), tritons (3H), helions (3He), alphas (4He)
- Low-density, low-temperature limit:
Virial expansion, non-interacting nuclides, quantum condensates
- Transition to higher densities:
Medium effects, quasiparticles. Interpolation between Beth-Uhlenbeck and DBHF / RMF
- Cluster formation (correlations) vs. mean field:
Consistent quantum-statistical approach

Outline

- Schrödinger equation with medium corrections:
Self-energy and Pauli blocking
- Composition of the nuclear gas:
Generalized Beth-Uhlenbeck equation
- Quantum condensates:
Pairing and quartetting
- Composition and the EoS of nuclear matter
(astrophysics: supernovae explosions)
- Symmetry energy in the low-density region
(heavy ion collisions: cluster abundances)
- Cluster formation in dilute nuclei
(Hoyle state and THSR wave function)

Ideal mixture of reacting nuclides

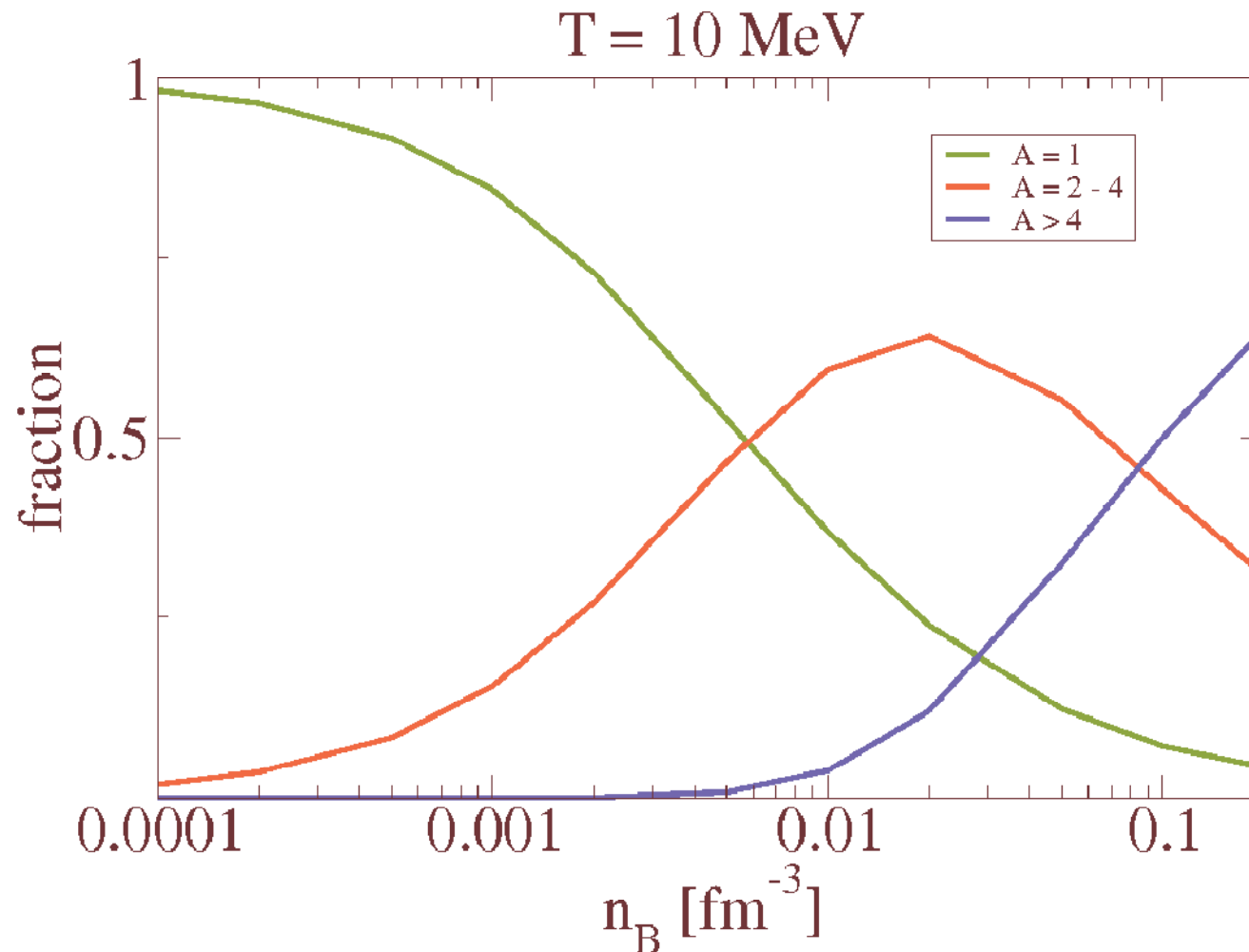
$$\begin{aligned} n_p(T, \mu_p, \mu_n) &= \frac{1}{V} \sum_{A,\nu,K} Z_A f_A \{ E_{A,\nu K} - Z_A \mu_p - (A - Z_A) \mu_n \} \\ n_n(T, \mu_p, \mu_n) &= \frac{1}{V} \sum_{A,\nu,K} (A - Z_A) f_A \{ E_{A,\nu K} - Z_A \mu_p - (A - Z_A) \mu_n \} \\ &\quad (\text{statistical multifragmentation}) \end{aligned}$$

mass number A ,
charge Z_A ,
energy $E_{A,\nu K}$,
 ν : internal quantum number,
 K : center of mass momentum

$$f_A(z) = \frac{1}{\exp(z/T) - (-1)^A}$$

Composition of symmetric matter

Ideal mixture of nuclides



Virial expansion

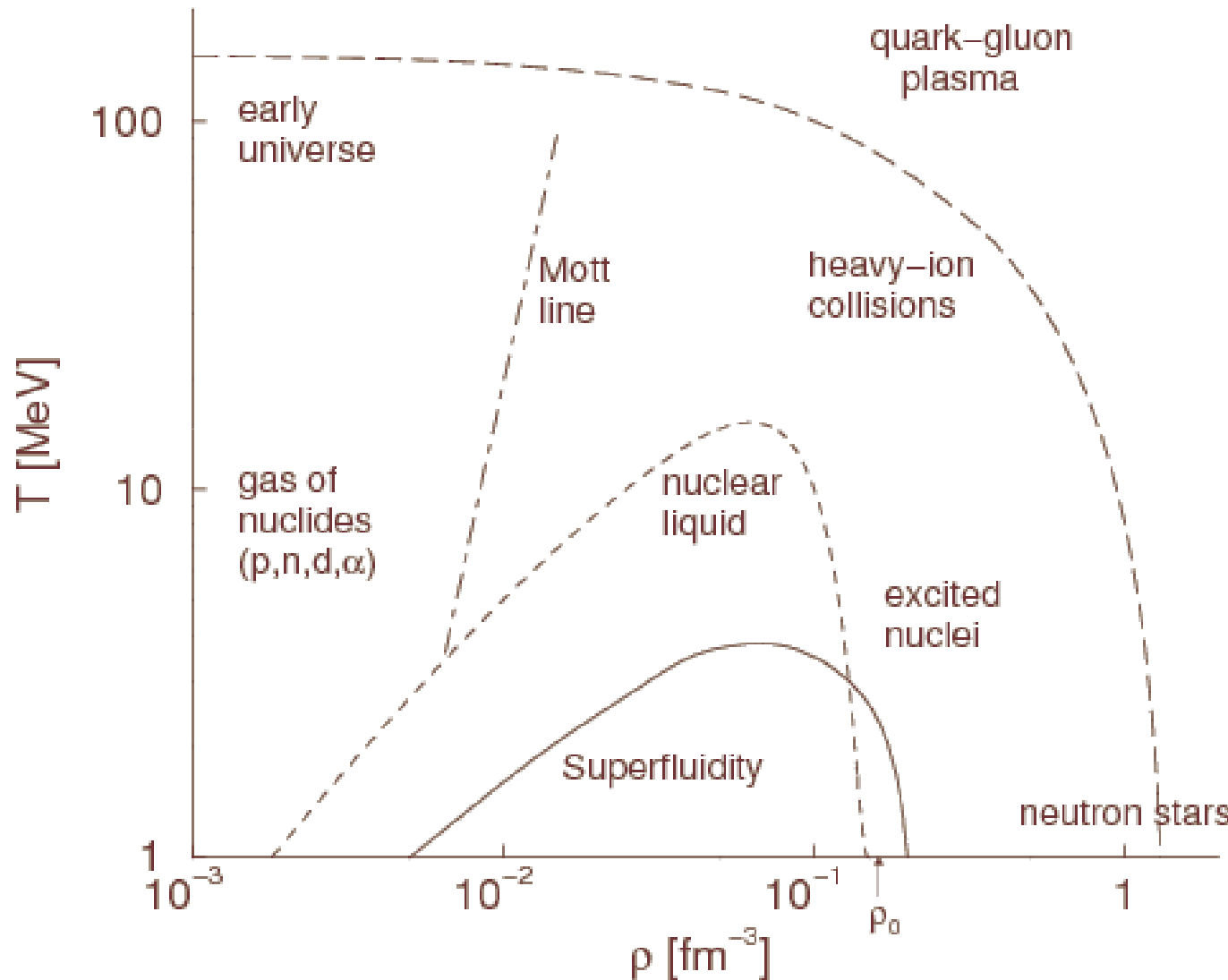
- excited nuclei
- resonances
- scattering phase shifts (no double counting)
- virial expansions
- quantum statistical approach

Particle clustering and Mott transition in nuclear matter at finite temperatures,
G. Röpke, M. Schmidt, L. Münchow, H. Schulz: NPA **399**, 587-602 (1983).

Generalized Beth-Uhlenbeck Approach for Hot Nuclear Matter,
M. Schmidt, G. Röpke, H. Schulz: Annals of Physics **202**, 57 - 99 (1990).

Cluster formation and the virial equation of state of low-density nuclear matter,
C. J. Horowitz and A. Schwenk, Nucl. Phys. **A 776**, 55 (2006).

Symmetric nuclear matter: Phase diagram



Nucleon-nucleon interaction

- general form:

$$V_\alpha(p, p') = \sum_{i,j=1}^N w_{\alpha i}(p) \lambda_{\alpha i j} w_{\alpha j}(p') \quad \text{uncoupled}$$

and

$$V_\alpha^{LL'}(p, p') = \sum_{i,j=1}^N w_{\alpha i}^L(p) \lambda_{\alpha i j} w_{\alpha j}^{L'}(p') \quad \text{coupled}$$

p, p' in- and outgoing relative momentum

α ... channel

N ... rank

$\lambda_{\alpha i j}$. coupling parameter

L, L' orbital angular momentum

Many-particle theory

- equilibrium correlation functions

e.g. equation of state $n(\beta, \mu) = \frac{1}{\Omega_0} \sum_1 \langle a_1^\dagger a_1 \rangle$

$$\text{density matrix } \langle a_1^\dagger a_1 \rangle = \int \frac{d\omega}{2\pi} e^{-i\omega t} f_1(\omega) A(1, 1', \omega)$$

- Spectral function

$$A(1, 1', \omega) = \text{Im} [G(1, 1', \omega + i\eta) - G(1, 1', \omega - i\eta)]$$

- Matsubara Green function

$$G(1, 1', iz_\nu), \quad z_\nu = \frac{\pi\nu}{\beta} + \mu, \quad \nu = \pm 1, \pm 3, \dots$$

$$1 \equiv \{\mathbf{p}_1, \sigma_1, c_1\}, \quad f_1(\omega) = \frac{1}{e^{\beta(\omega-\mu)} + 1}, \quad \Omega_0 = \text{volume}$$

Many-particle theory

- Dyson equation and self energy (homogeneous system)

$$G(1, iz_\nu) = \frac{1}{iz_\nu - E(1) - \Sigma(1, iz_\nu)}$$

- Evaluation of $\Sigma(1, iz_\nu)$:
perturbation expansion, diagram representation

$$A(1, \omega) = \frac{2\text{Im } \Sigma(1, \omega + i0)}{[\omega - E(1) - \text{Re } \Sigma(1, \omega)]^2 + [\text{Im } \Sigma(1, \omega + i0)]^2}$$

approximation for self energy \longrightarrow approximation for equilibrium correlation functions

alternatively: simulations, path integral methods

Different approximations

- Expansion for small $\text{Im } \Sigma(1, \omega + i\eta)$

$$A(1, \omega) \approx \frac{2\pi\delta(\omega - E^{\text{quasi}}(1))}{1 - \frac{d}{dz}\text{Re } \Sigma(1, z)|_{z=E^{\text{quasi}}-\mu_1}} - 2\text{Im } \Sigma(1, \omega + i\eta) \frac{d}{d\omega} \frac{P}{\omega + \mu_1 - E^{\text{quasi}}(1)}$$

quasiparticle energy $E^{\text{quasi}}(1) = E(1) + \text{Re } \Sigma(1, \omega)|_{\omega=E^{\text{quasi}}}$

- chemical picture: bound states $\hat{=}$ new species

summation of ladder diagrams, Bethe-Salpeter equation



Medium effects: Quasiparticle approximation

- Skyrme
- relativistic mean field (RMF)
- Lagrangian: non-linear sigma
- TM1 parameters
- Single particle modifications
- energy shift, effective mass
- DD-RMF [S.Typel, Phys. Rev. C **71**, 064301 (2007)]:
expansion of the scalar field and the vector fields
in powers of proton/neutron densities
- Dirac-Brueckner Hartree Fock (DBHF)

Quasiparticle energy shifts

Comparison of different approximations, BonnA separable interaction potential.

Full line - generalized Beth-Uhlenbeck approach,

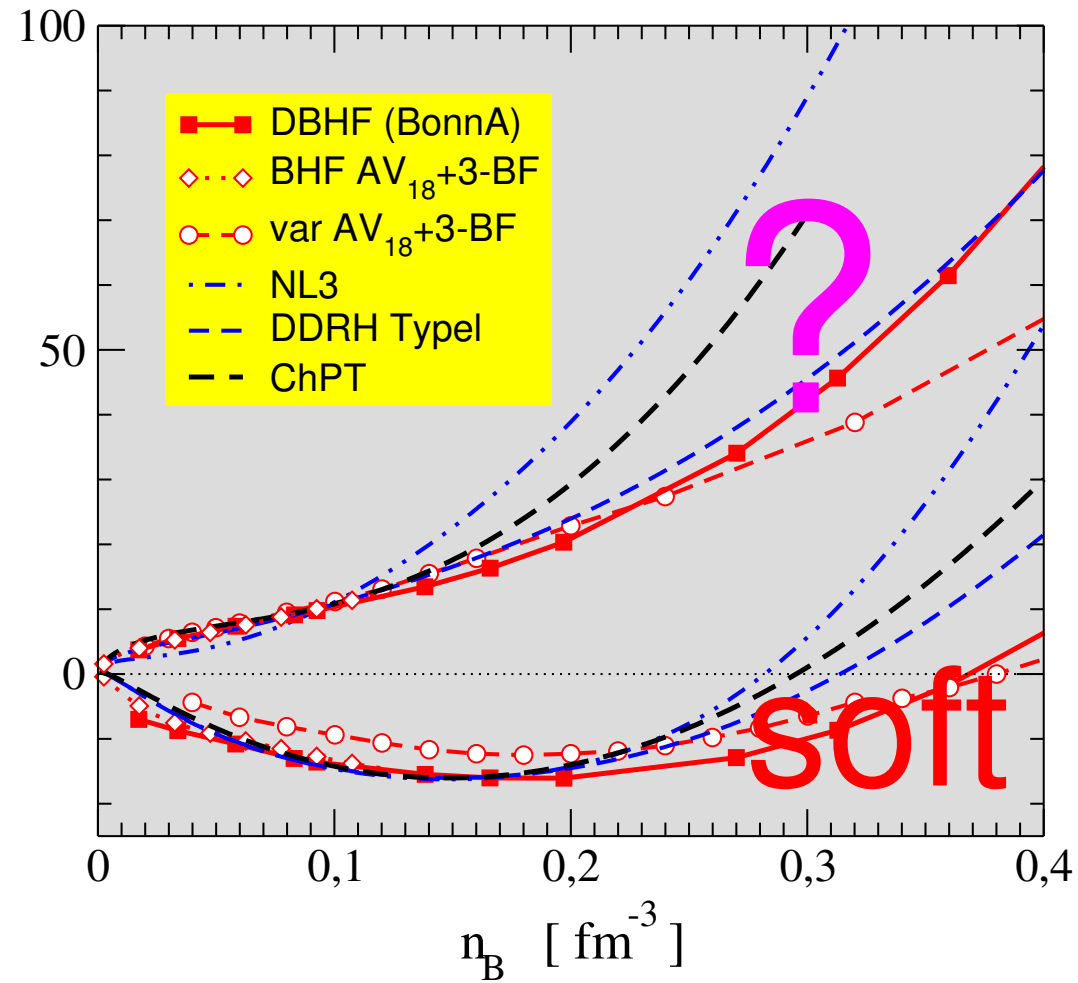
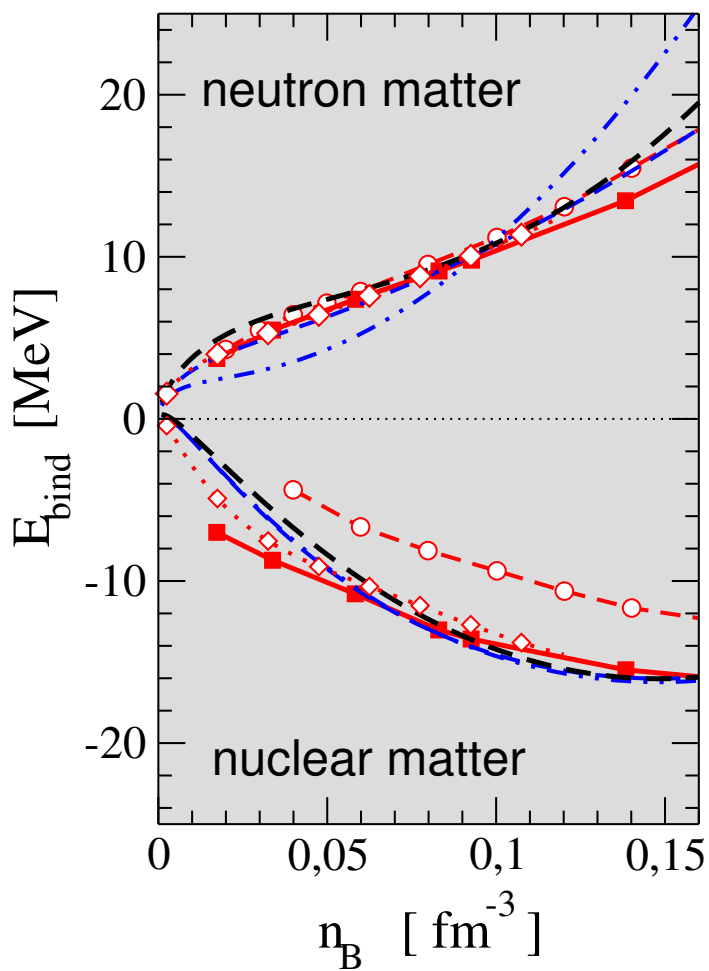
dotted line - the same but the Pauli operator

$(1 - f_1)(1 - f_1)$ instead of $(1 - f_1 - f_1)$,

dashed line - Brueckner-Bethe-Goldstone calculation with the Pauli operator $(1 - f_1)(1 - f_1)$.

QuickTime™ and a
TIFF (LZW) decompressor
are needed to see this picture.

Quasiparticle picture: RMF and DBHF



J.Margueron et al., PRC 76, 034309 (2007)

Different approximations

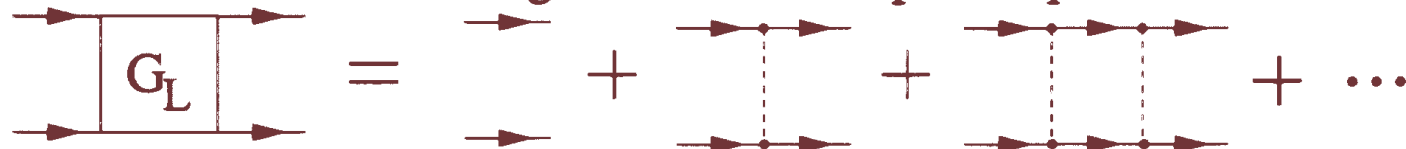
- Expansion for small $\text{Im } \Sigma(1, \omega + i\eta)$

$$A(1, \omega) \approx \frac{2\pi\delta(\omega - E^{\text{quasi}}(1))}{1 - \frac{d}{dz} \text{Re } \Sigma(1, z)|_{z=E^{\text{quasi}}-\mu_1}} - 2\text{Im } \Sigma(1, \omega + i\eta) \frac{d}{d\omega} \frac{P}{\omega + \mu_1 - E^{\text{quasi}}(1)}$$

quasiparticle energy $E^{\text{quasi}}(1) = E(1) + \text{Re } \Sigma(1, \omega)|_{\omega=E^{\text{quasi}}}$

- chemical picture: bound states $\hat{=}$ new species

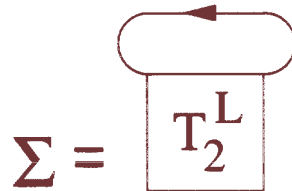
summation of ladder diagrams, Bethe-Salpeter equation



Different approximations

low density limit:

$$G_2^L(12, 1'2', i\lambda) = \sum_{n\mathbf{P}} \Psi_{n\mathbf{P}}(12) \frac{1}{i\omega_\lambda - E_{n\mathbf{P}}} \Psi_{n\mathbf{P}}^*(12)$$



$$\begin{aligned} n(\beta, \mu) &= \sum_1 f_1(E^{\text{quasi}}(1)) + \sum_{2,n\mathbf{P}}^{\text{bound}} g_{12}(E_{n\mathbf{P}}) \\ &+ \sum_{2,n\mathbf{P}} \int_0^\infty dk \delta_{\mathbf{k}, \mathbf{p}_1 - \mathbf{p}_2} g_{12}(E^{\text{quasi}}(1) + E^{\text{quasi}}(2)) 2 \sin^2 \delta_n(k) \frac{1}{\pi} \frac{d}{dk} \delta_n(k) \end{aligned}$$

- generalized Beth-Uhlenbeck formula
correct low density/low temperature limit:
mixture of free particles and bound clusters

Effective wave equation for the deuteron in matter

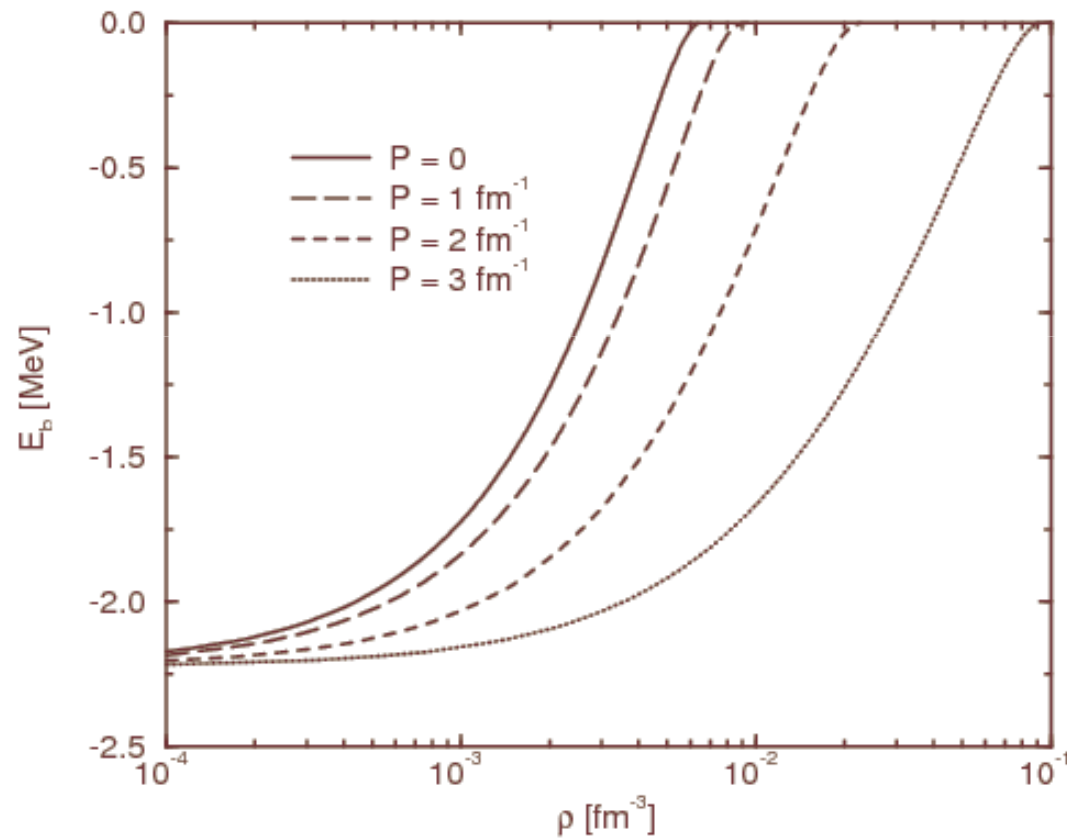
$$\left(\frac{p_1^2}{2m_1} + \frac{p_2^2}{2m_2} \right) \Psi_{n,P}(p_1, p_2) + \sum_{p_1', p_2'} (1 - f_{p_1} - f_{p_2}) V(p_1, p_2; p_1', p_2') \Psi_{n,P}(p_1', p_2') = E_{n,P} \Psi_{n,P}(p_1, p_2)$$

Fermi distribution function

$$f_p = \left[e^{(p^2/2m - \mu)/k_B T} + 1 \right]^{-1}$$

BEC-BCS crossover: Alm et al., 1993

Deuterons in nuclear matter



$T=10 \text{ MeV}$, P : center of mass momentum

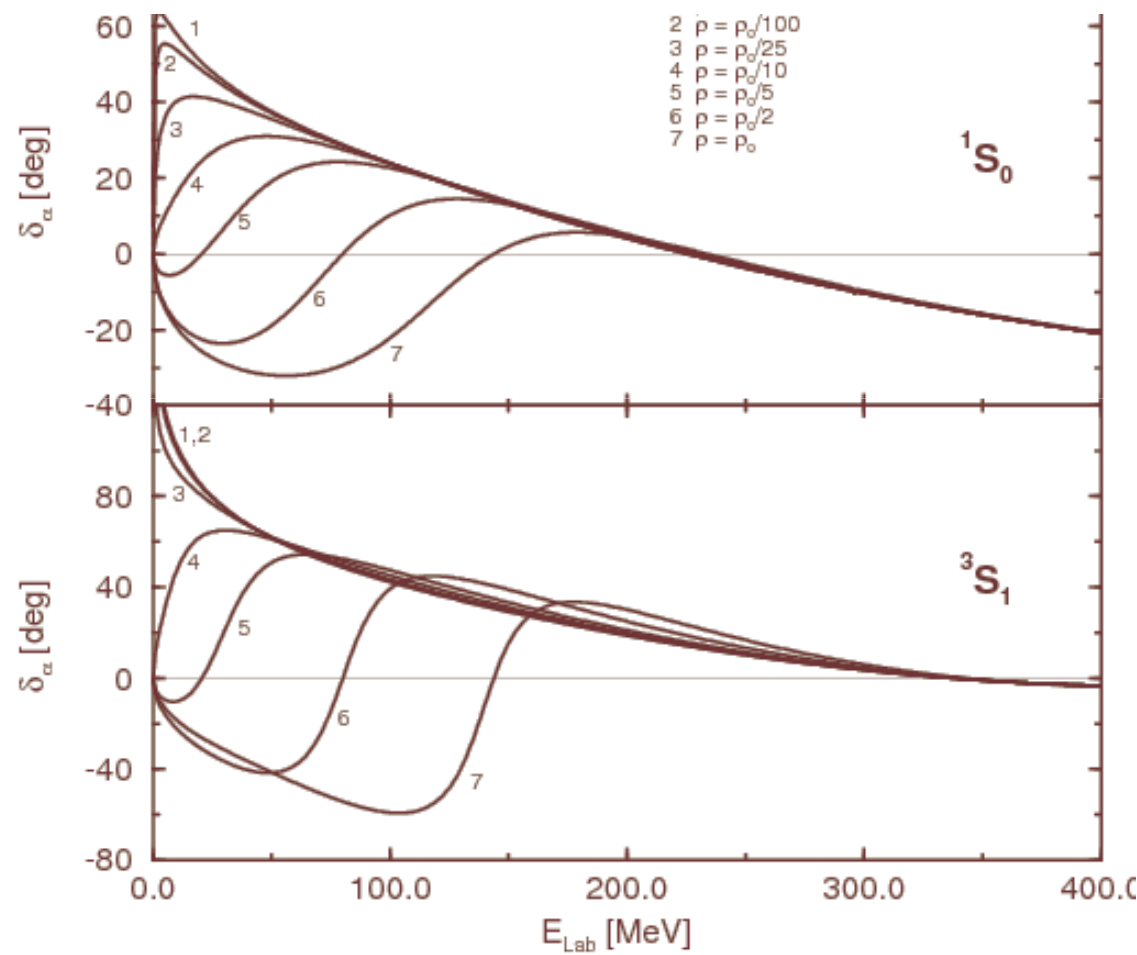
Deuteron quasiparticle properties

$$E_d^{\text{qu}}(P) = E_d^{\text{free}} + \Delta E_d + \frac{\hbar}{2m_d^*} P^2 + O(P^4)$$
$$E_d^{\text{free}} = -2.225 \text{ MeV}$$

$$\Delta E_d^{\text{Pauli}}(T, n_B, \alpha) = \delta E_d^{(0)}(T, \alpha) n_B + O(n_B^2)$$
$$\frac{m_d}{m_d}(T, n_B, \alpha) = 1 + \delta m_d^{(0)}(T, \alpha) n_B + O(n_B^2)$$

T [MeV]	delta E [MeV fm^3]	delta m^* [fm^3]
10	364.3	21.3
4	712.9	87.1

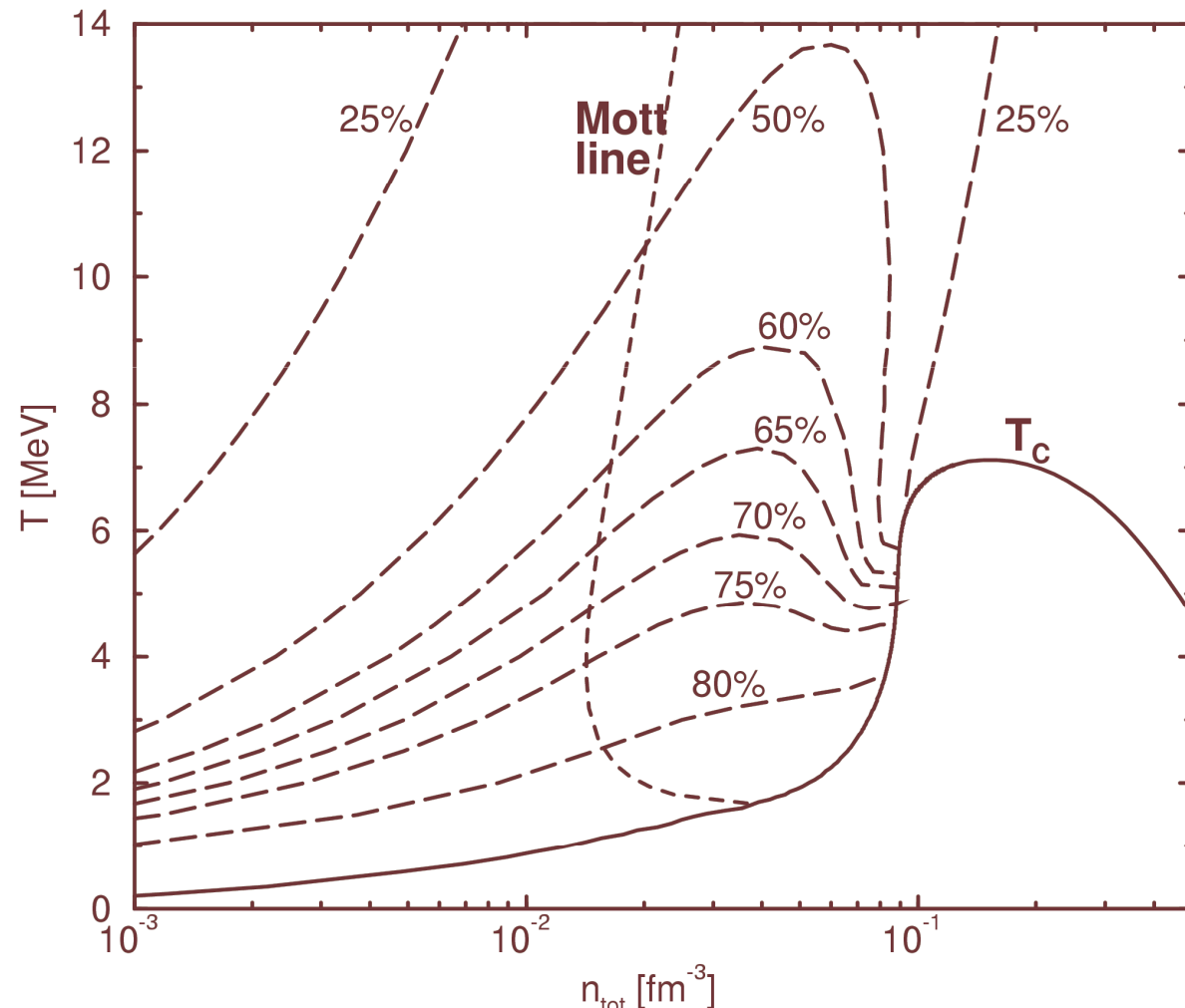
Scattering phase shifts in matter



Composition of symmetric nuclear matter

Fraction of correlated matter
(virial expansion,
Generalized Beth-Uhlenbeck approach,
contribution of bound states,
of scattering states,
phase shifts)

H. Stein et al.,
Z. Phys. A351, 259 (1995)



Cluster decomposition of the self-energy

$$\Sigma_1 = \text{Diagram } T_2 + \text{Diagram } T_3 + \text{Diagram } T_4 + \dots$$

The diagram illustrates the cluster decomposition of the self-energy Σ_1 . It is represented as a sum of diagrams, starting with a basic semi-circular form and adding more complex components. The first term is a dashed semi-circle with a central dot. Subsequent terms are represented by solid semi-circles containing rectangles labeled T_2 , T_3 , and T_4 , respectively. Each T_n consists of a rectangle with a semi-circular arc above it, and a dot at the top center of the rectangle. The ellipsis at the end of the series indicates that the decomposition continues for higher-order terms.

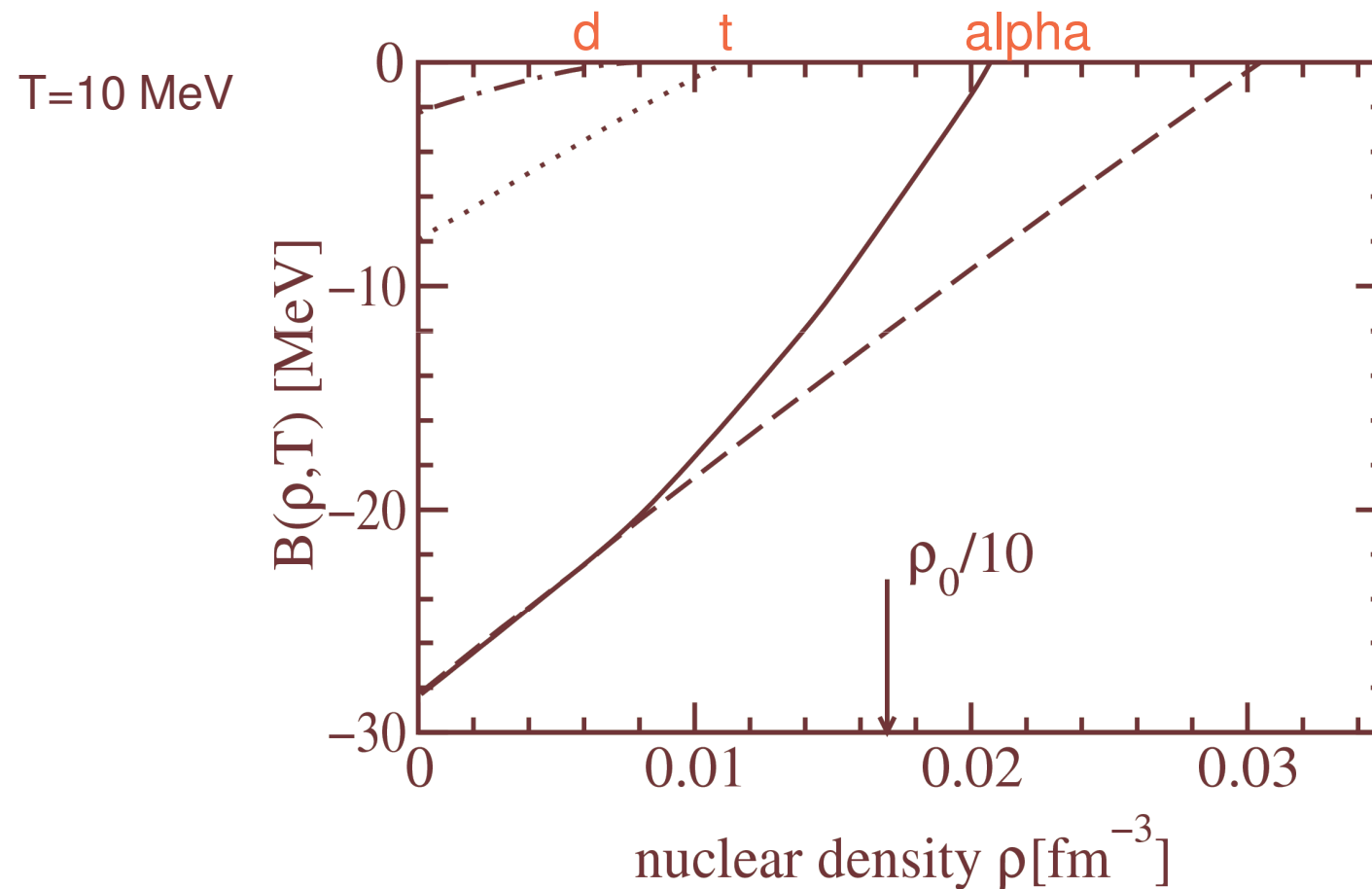
Few-particle Schoedinger equation in a dense medium

Four-particle Schrödinger equation with medium effects

$$\begin{aligned} & [E^{\text{HF}}(p_1) + E^{\text{HF}}(p_2) + E^{\text{HF}}(p_3) + E^{\text{HF}}(p_4)] \psi_{nP}(p_1, p_2, p_3, p_4) \\ & + \sum_{p'_1 p'_2 p'_3 p'_4} \left\{ \left[1 - \frac{f(p_1)}{f(p'_1)} - \frac{f(p_2)}{f(p'_2)} \right] V(p_1 p_2, p'_1 p'_2) \delta_{p_3 p'_3} \delta_{p_4 p'_4} \right. \\ & \quad + \left[1 - \frac{f(p_1)}{f(p'_1)} - \frac{f(p_3)}{f(p'_3)} \right] V(p_1 p_3, p'_1 p'_3) \delta_{p_2 p'_2} \delta_{p_4 p'_4} \\ & \quad \left. + \text{permutations} \right\} \psi_{nP}(p'_1, p'_2, p'_3, p'_4) \\ & = E_{nP} \psi_{nP}(p_1, p_2, p_3, p_4) \end{aligned}$$

In-medium shift of binding energies of clusters

Solution of the Faddeev-Yakubovski equation with Pauli blocking



Composition of dense nuclear matter

$$n_p(T, \mu_p, \mu_n) = \frac{1}{V} \sum_{A,\nu,K} Z_A f_A \{ E_{A,\nu K} - Z_A \mu_p - (A - Z_A) \mu_n \}$$
$$n_n(T, \mu_p, \mu_n) = \frac{1}{V} \sum_{A,\nu,K} (A - Z_A) f_A \{ E_{A,\nu K} - Z_A \mu_p - (A - Z_A) \mu_n \}$$

mass number A ,
charge Z_A ,
energy $E_{A,\nu K}$,
 ν : internal quantum number,

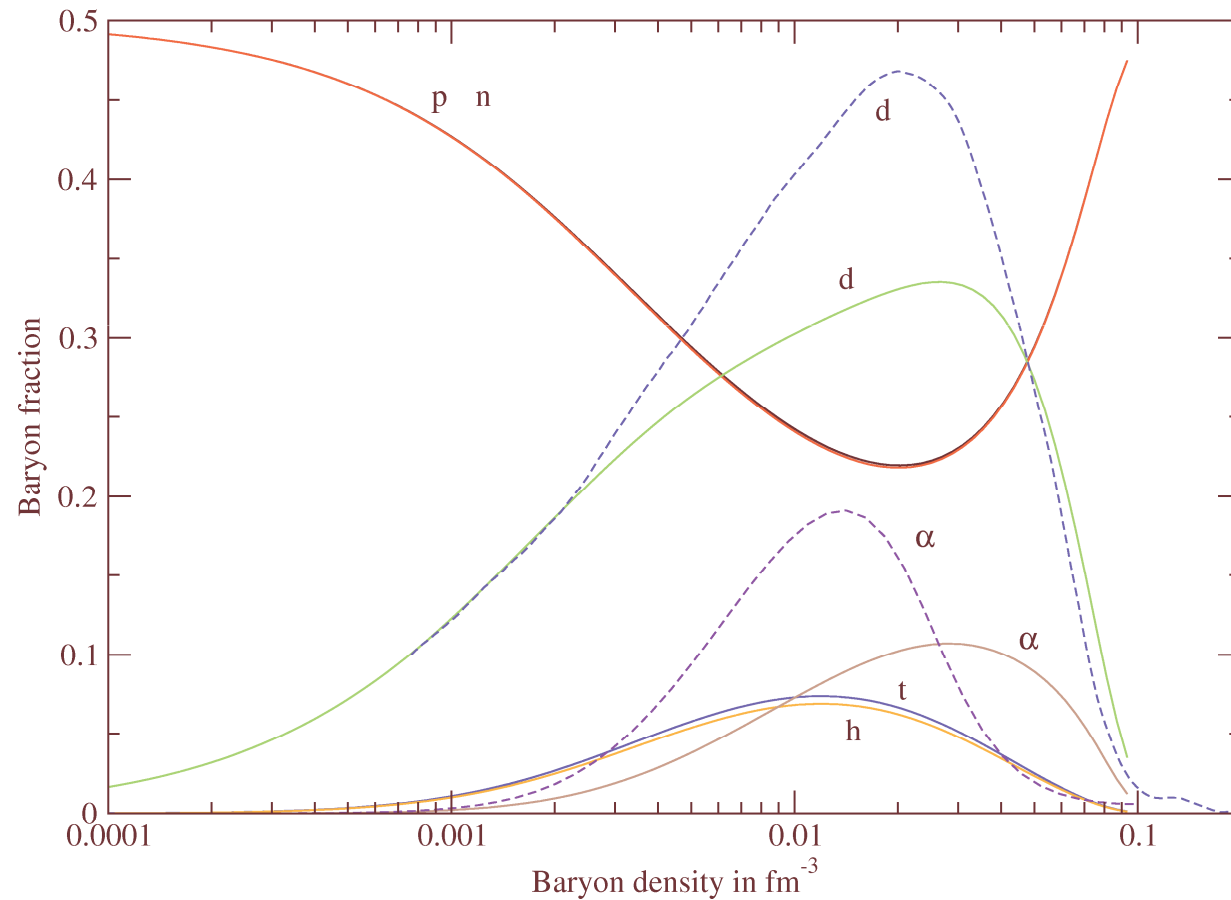
$$f_A(z) = \frac{1}{\exp(z/T) - (-1)^A}$$

- Inclusion of excited states and continuum correlations
- Medium effects:
self-energy and Pauli blocking shifts of binding energies,
Coulomb corrections due to screening (Wigner-Seitz, Debye)

Composition of symmetric nuclear matter

T=10 MeV

G.Ropke, A.Grigo, K. Sumiyoshi, Hong Shen,
Phys.Part.Nucl.Lett. **2**, 275 (2005)

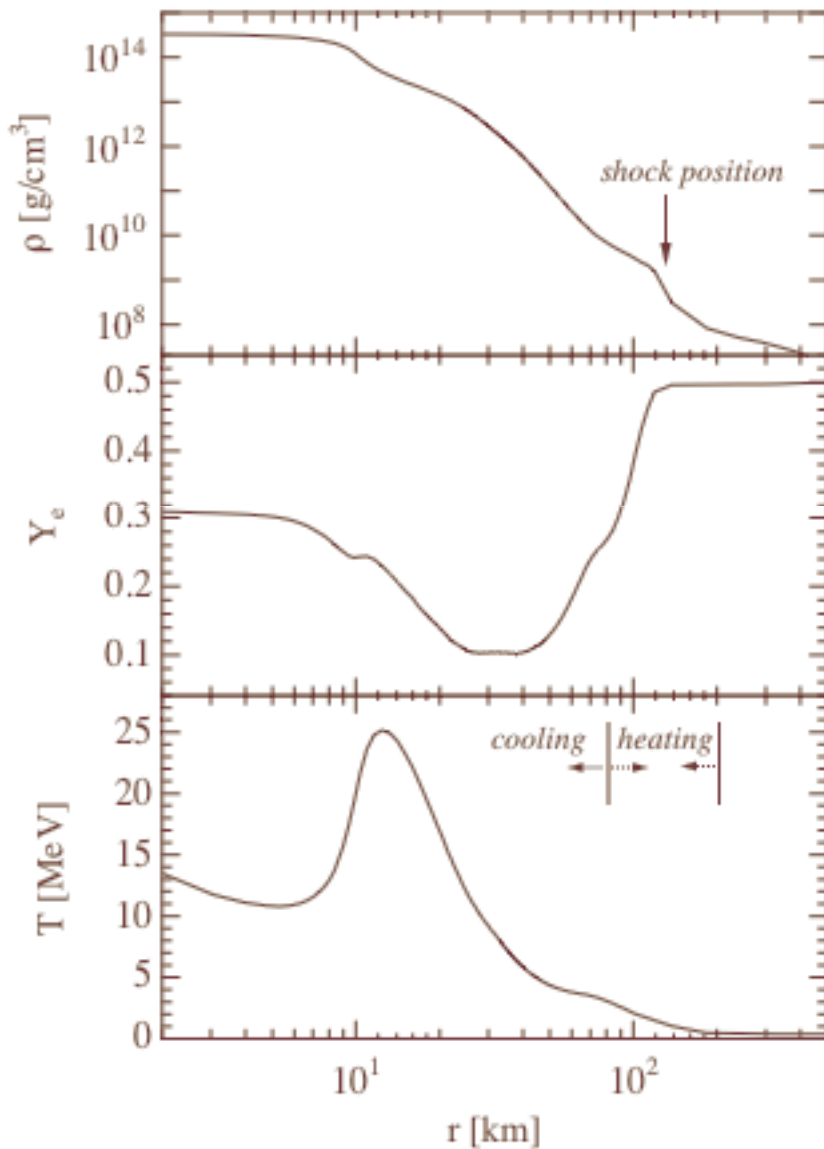


Light Cluster Abundances

QuickTime™ and a
TIFF (LZW) decompressor
are needed to see this picture.

S. Typel, 2007

Core-collapse supernovae

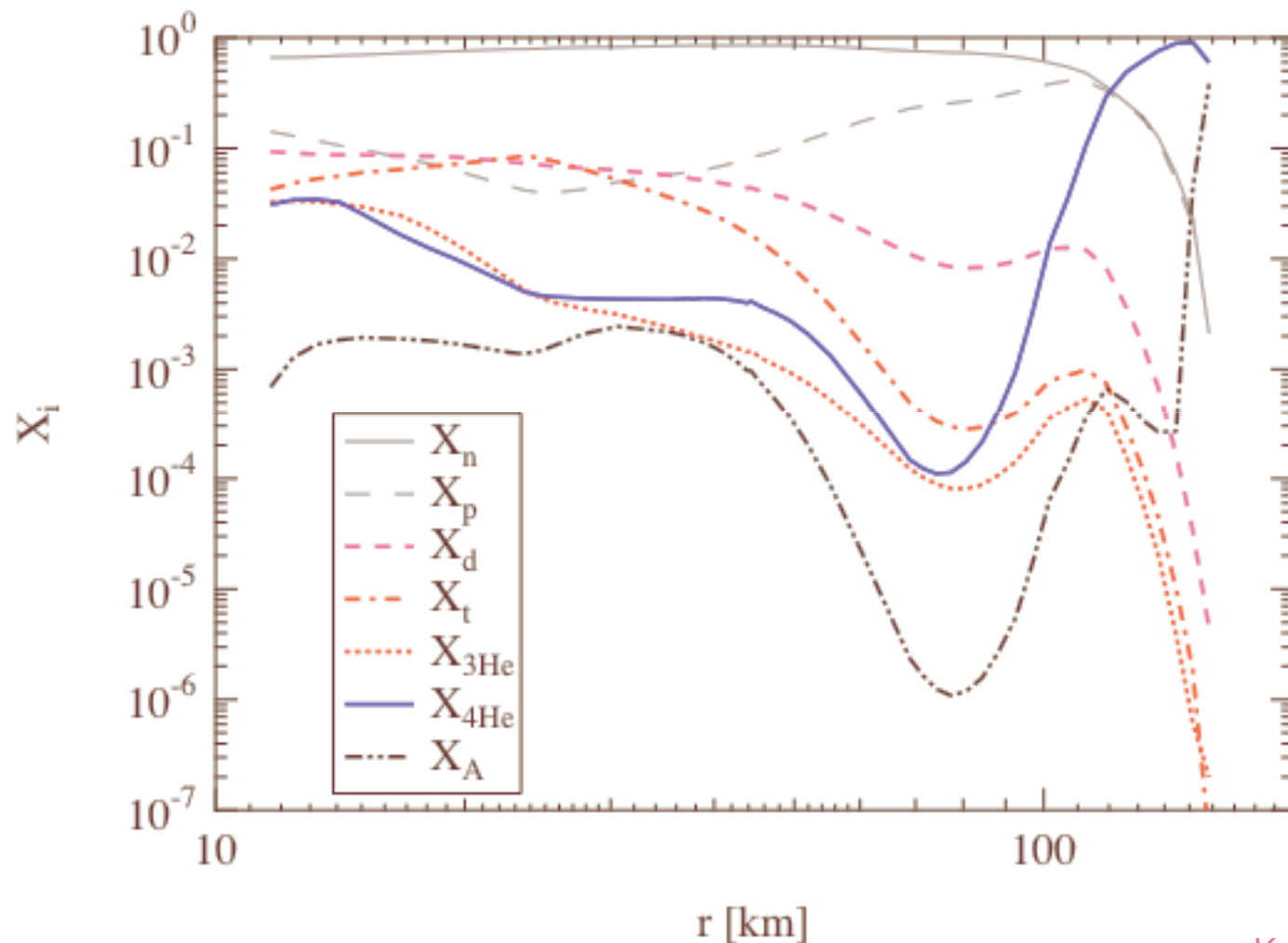


Density,
electron fraction, and
temperature profile
of a 15 solar mass supernova
at 150 ms after core bounce
as function of the radius.

Influence of cluster formation
on neutrino emission
in the cooling region and
on neutrino absorption
in the heating region ?

K.Sumiyoshi et al.,
Astrophys.J. **629**, 922 (2005)

Composition of supernova core



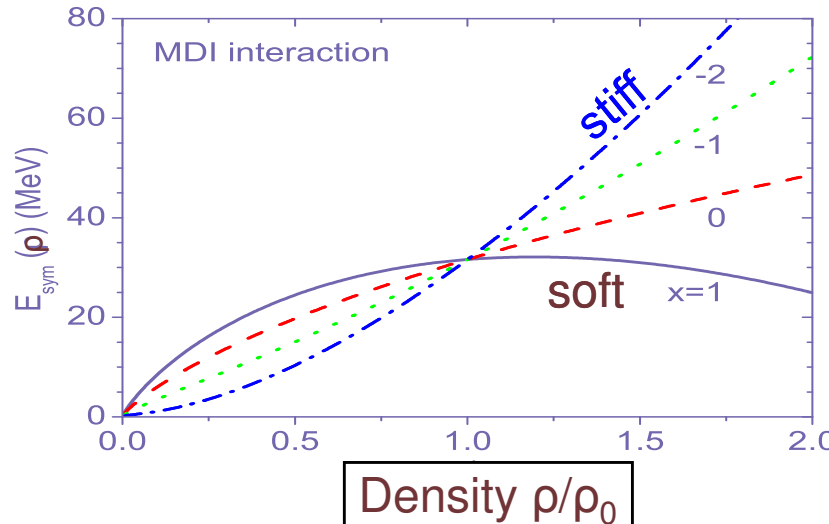
Mass fraction X of light clusters for a post-bounce supernova core

K. Sumiyoshi, G. R.,
PRC 77, 055804 (08)

Symmetry energy of a low density nuclear gas

- L. W. Chen, C. M. Ko, and B. A. Li,
Phys. Rev. Lett. **94**, 032701 (2005).
- T. Klähn *et al.*,
Phys. Rev. C **74**, 035802 (2006).
- C. J. Horowitz and A. Schwenk,
Nucl. Phys. **A 776**, 55 (2006).
- S. Kowalski *et al.*,
Phys. Rev. C **75**, 014601 (2007).

Symmetry energy and single nucleon potential used in the IBUU04 transport model



The x parameter is introduced to mimic various predictions by different microscopic Nuclear many-body theories using different Effective interactions

Single nucleon potential within the HF approach using a modified Gogny force:

$$U(\rho, \delta, \bar{p}, \tau, x) = A_u(x) \frac{\rho_\tau}{\rho_0} + A_l(x) \frac{\rho_\tau}{\rho_0} + B \left(\frac{\rho}{\rho_0} \right)^\sigma (1 - x \delta^2) - 8 \tau x \frac{B}{\sigma + 1} \frac{\rho^{\sigma-1}}{\rho_0^\sigma} \delta \rho_\tau + \frac{2C_{\tau,\tau}}{\rho_0} \int d^3 p' \frac{f_\tau(r, p')}{1 + (p - p')^2 / \Lambda^2} + \frac{2C_{\tau,\tau'}}{\rho_0} \int d^3 p' \frac{f_{\tau'}(r, p')}{1 + (p - p')^2 / \Lambda^2}$$

$$\tau, \tau' = \pm \frac{1}{2}, A_l(x) = -121 + \frac{2Bx}{\sigma + 1}, A_u(x) = -96 - \frac{2Bx}{\sigma + 1}, K_0 = 211 \text{ MeV}$$

The momentum dependence of the nucleon potential is a result of the non-locality of nuclear effective interactions and the Pauli exclusion principle

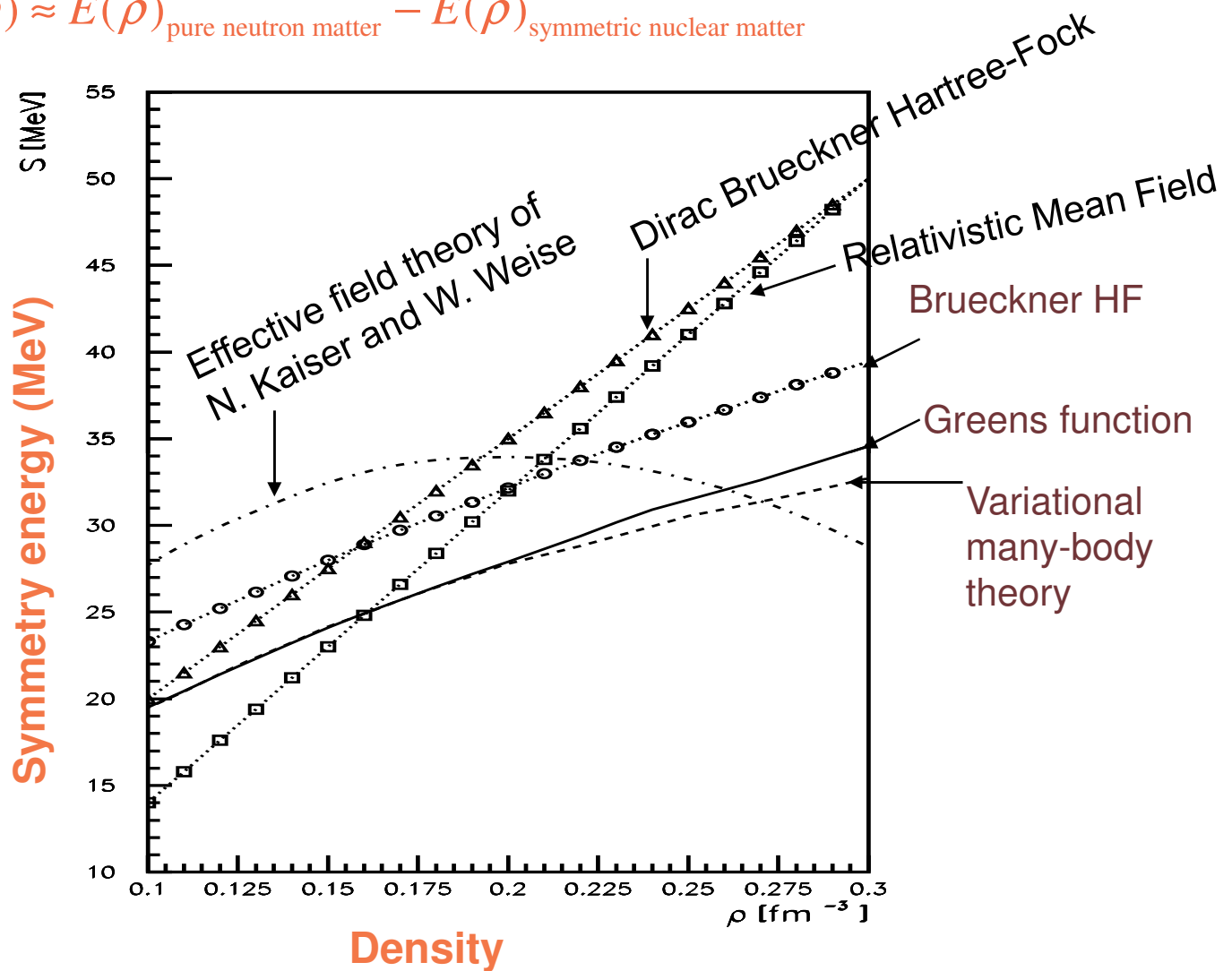
C.B. Das, S. Das Gupta, C. Gale and B.A. Li, PRC 67, 034611 (2003).

B.A. Li, C.B. Das, S. Das Gupta and C. Gale, PRC 69, 034614; NPA 735, 563 (2004).

$E_{sym}(\rho)$ predicted by microscopic many-body theories

EOS: $E(\rho, \delta) = E_0(\rho, 0) + E_{sym}(\rho)\delta^2 + o(\delta^4)$, where $\delta \equiv (\rho_n - \rho_p)/\rho$

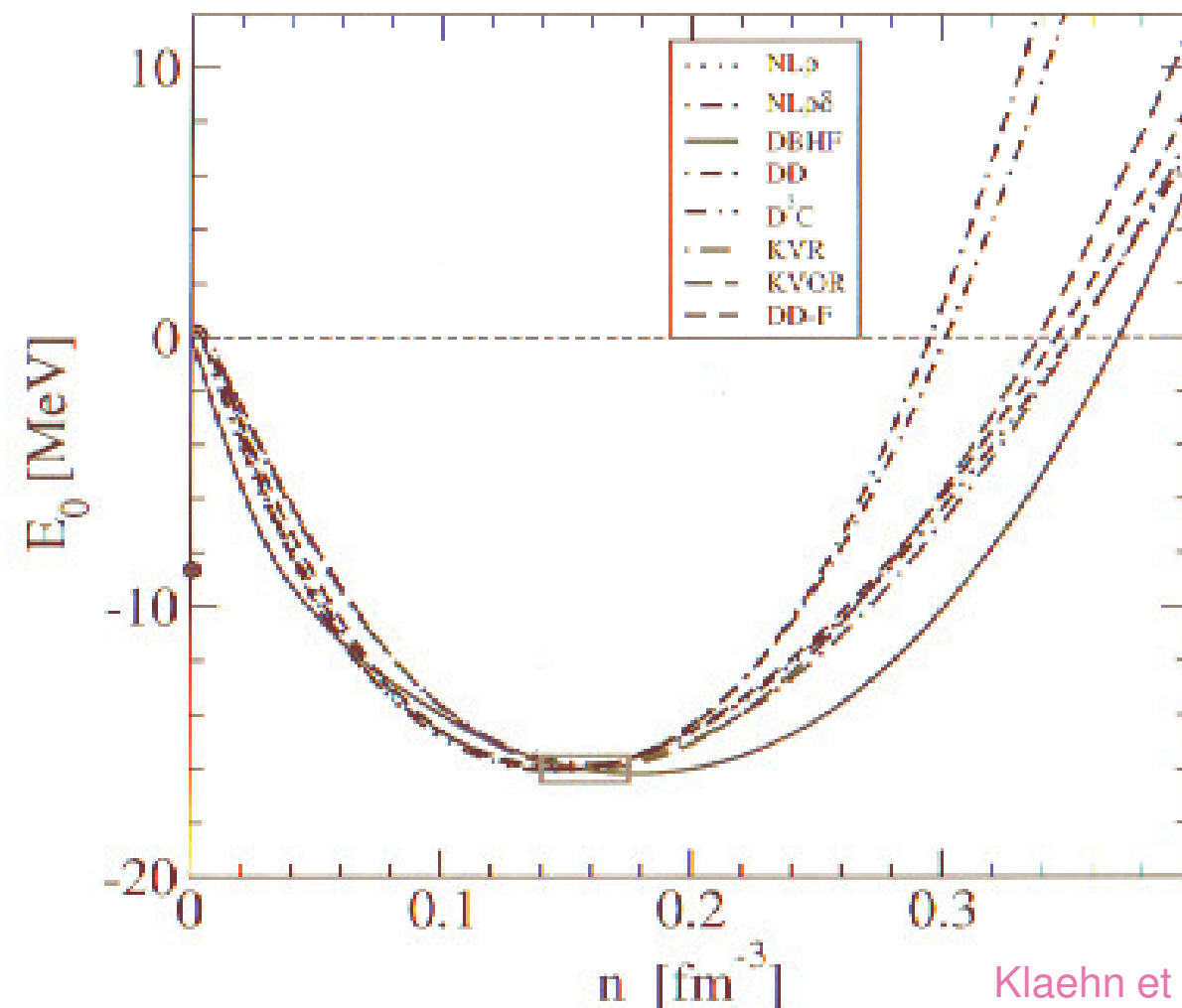
$$E_{sym}(\rho) \approx E(\rho)_{\text{pure neutron matter}} - E(\rho)_{\text{symmetric nuclear matter}}$$



A.E. L. Dieperink, Y. Dewulf, D. Van Neck, M. Waroquier and V. Rodin, Phys. Rev. C68 (2003) 064307

Quasiparticle approximation for nuclear matter

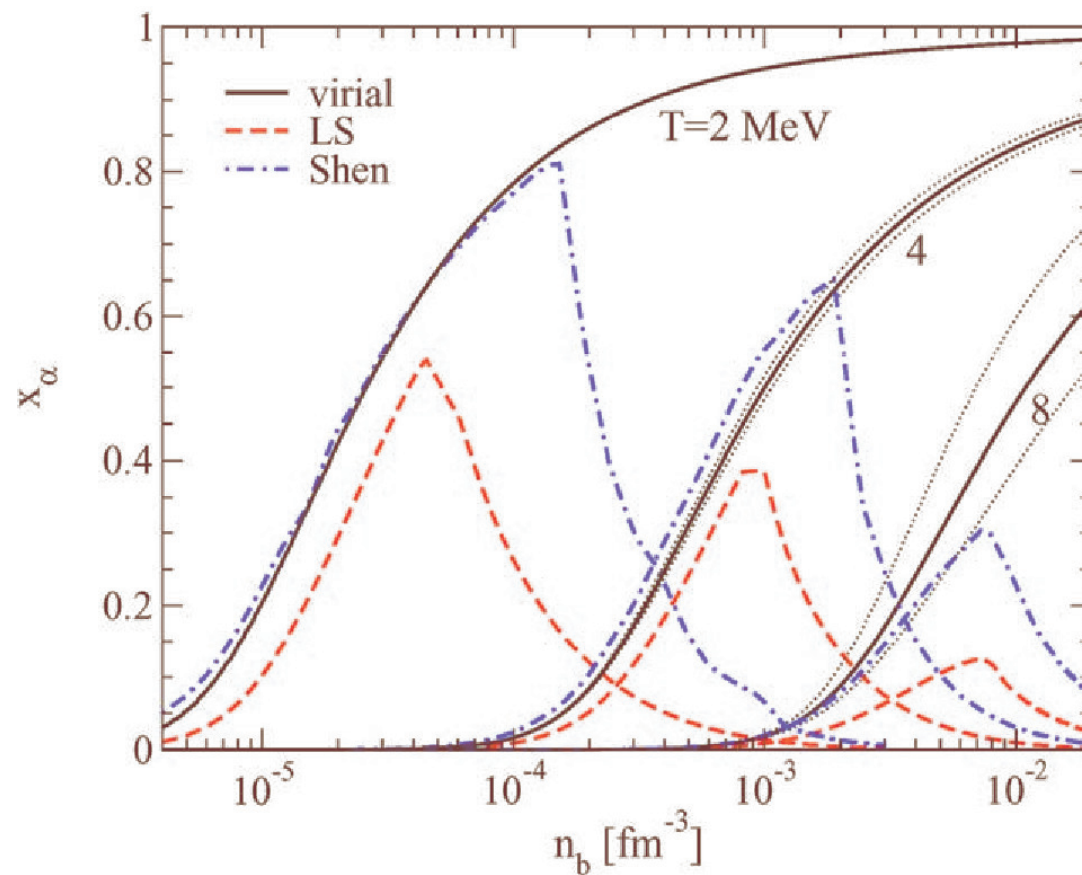
Equation of state for symmetric matter



Klaehn et al., PRC 74, 035802 (06)

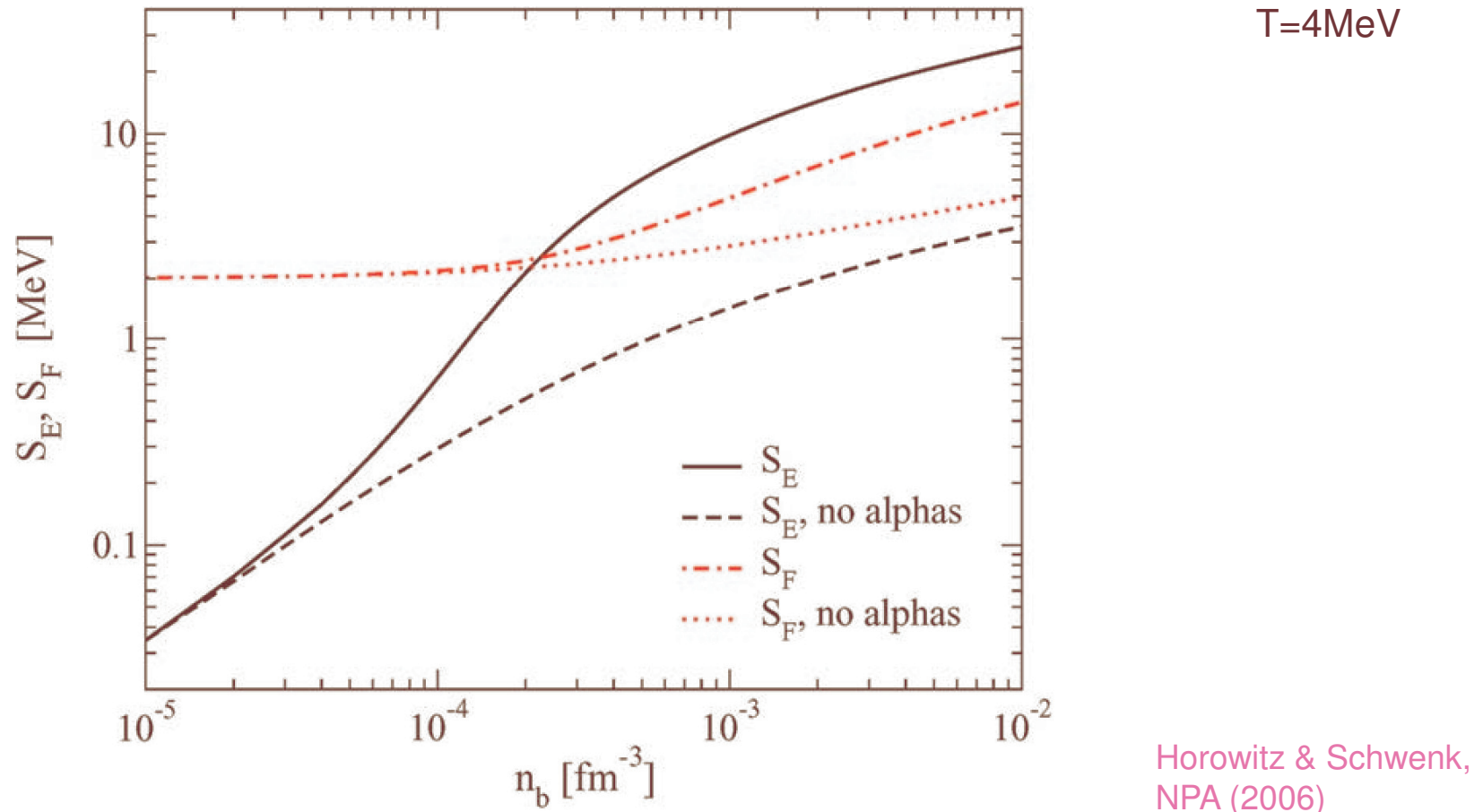
Alpha-particle fraction in the low-density limit

symmetric matter, $T=2, 4, 8$ MeV



C.J.Horowitz, A.Schwenk, Nucl. Phys. A **776**, 55 (2006)

Symmetry energy and symmetry free energy



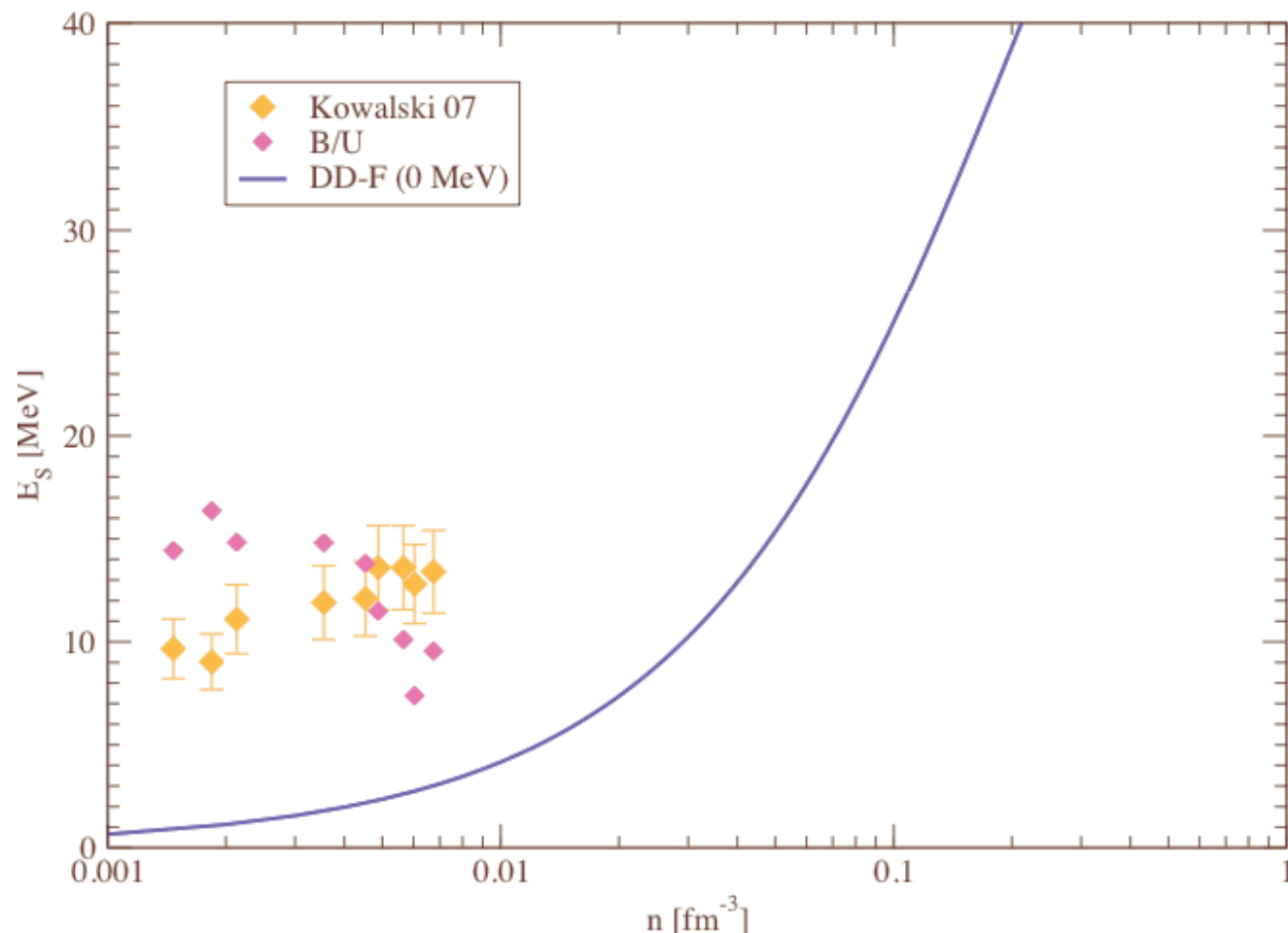
Horowitz & Schwenk,
NPA (2006)

Free and Internal Symmetry Energy

QuickTime™ and a
TIFF (LZW) decompressor
are needed to see this picture.

Symmetry energy

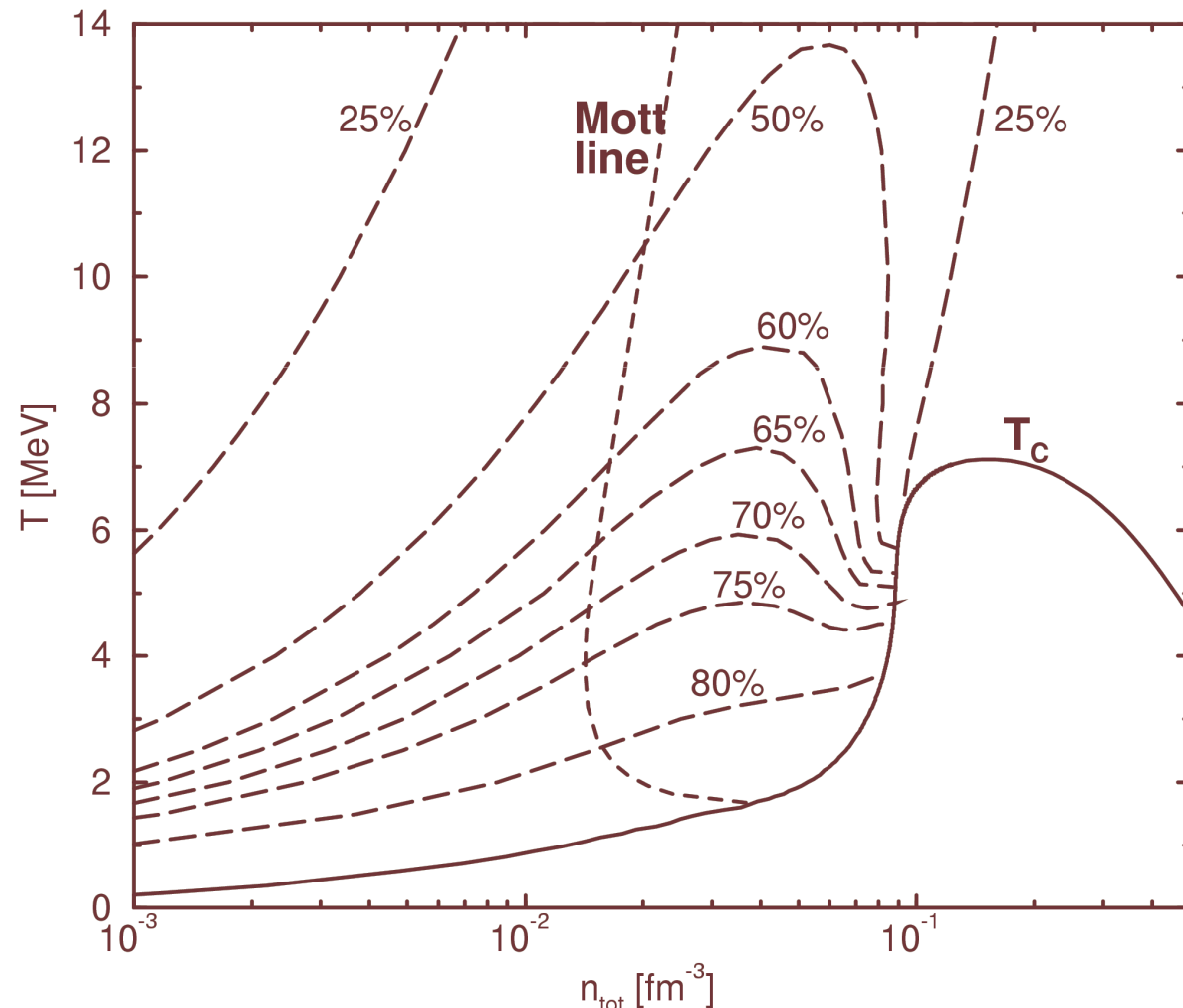
Heavy-ion collisions, spectra of emitted clusters,
temperature (3 - 10 MeV), free energy



Composition of symmetric nuclear matter

Fraction of correlated matter
(virial expansion,
Generalized Beth-Uhlenbeck approach,
contribution of bound states,
of scattering states,
phase shifts)

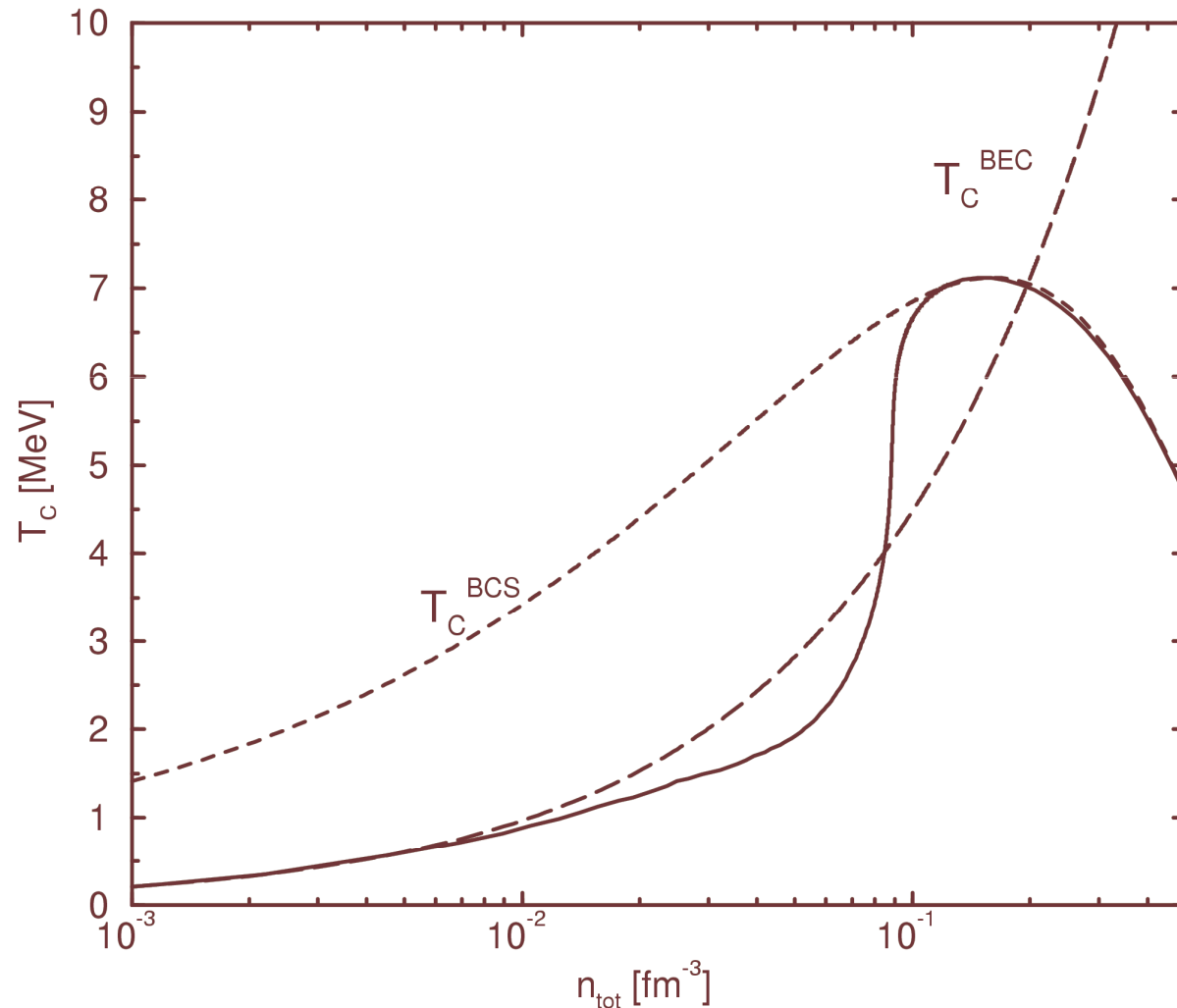
H. Stein et al.,
Z. Phys. A351, 259 (1995)



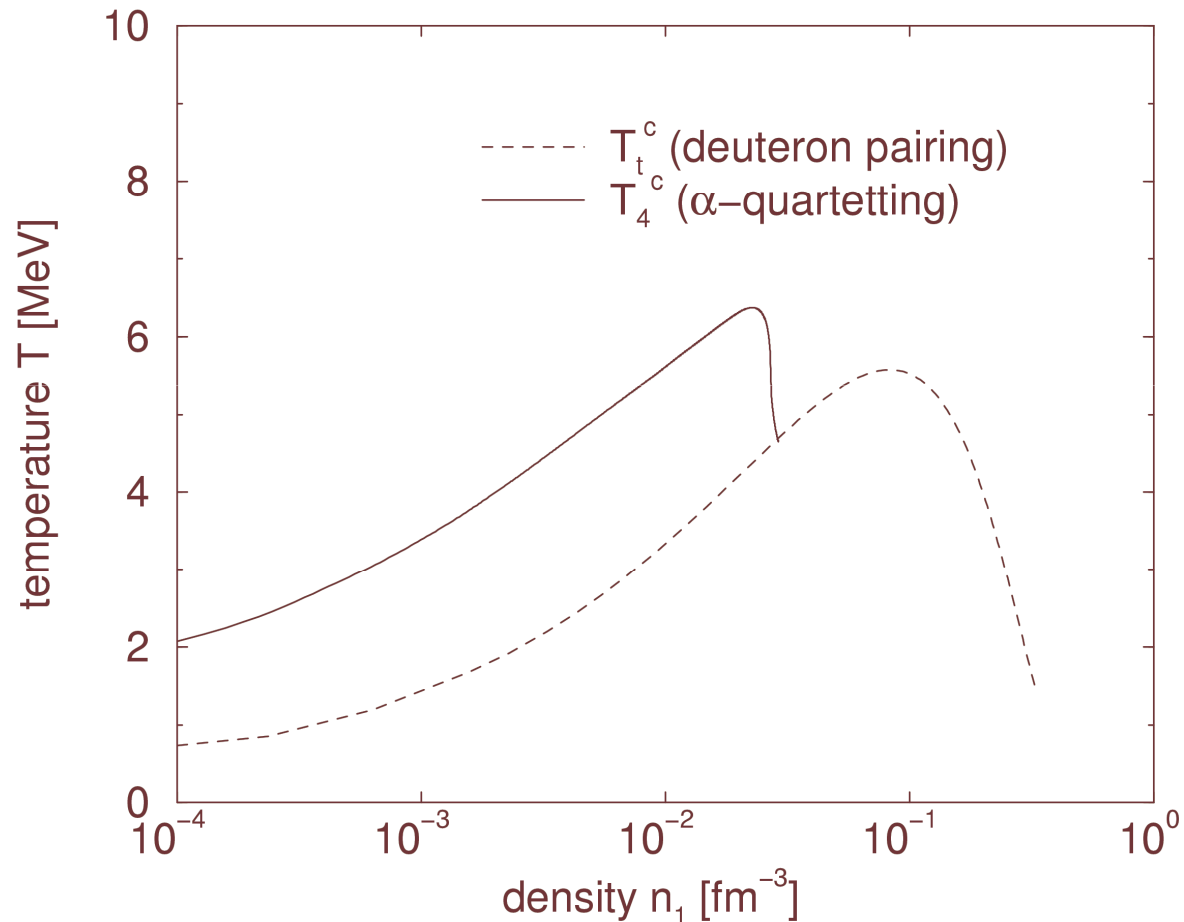
Quantum condensate

Bose-Einstein-
Condensation
of deuterons
(BEC)

Bardeen-Cooper
Schrieffer
pairing
(BCS)

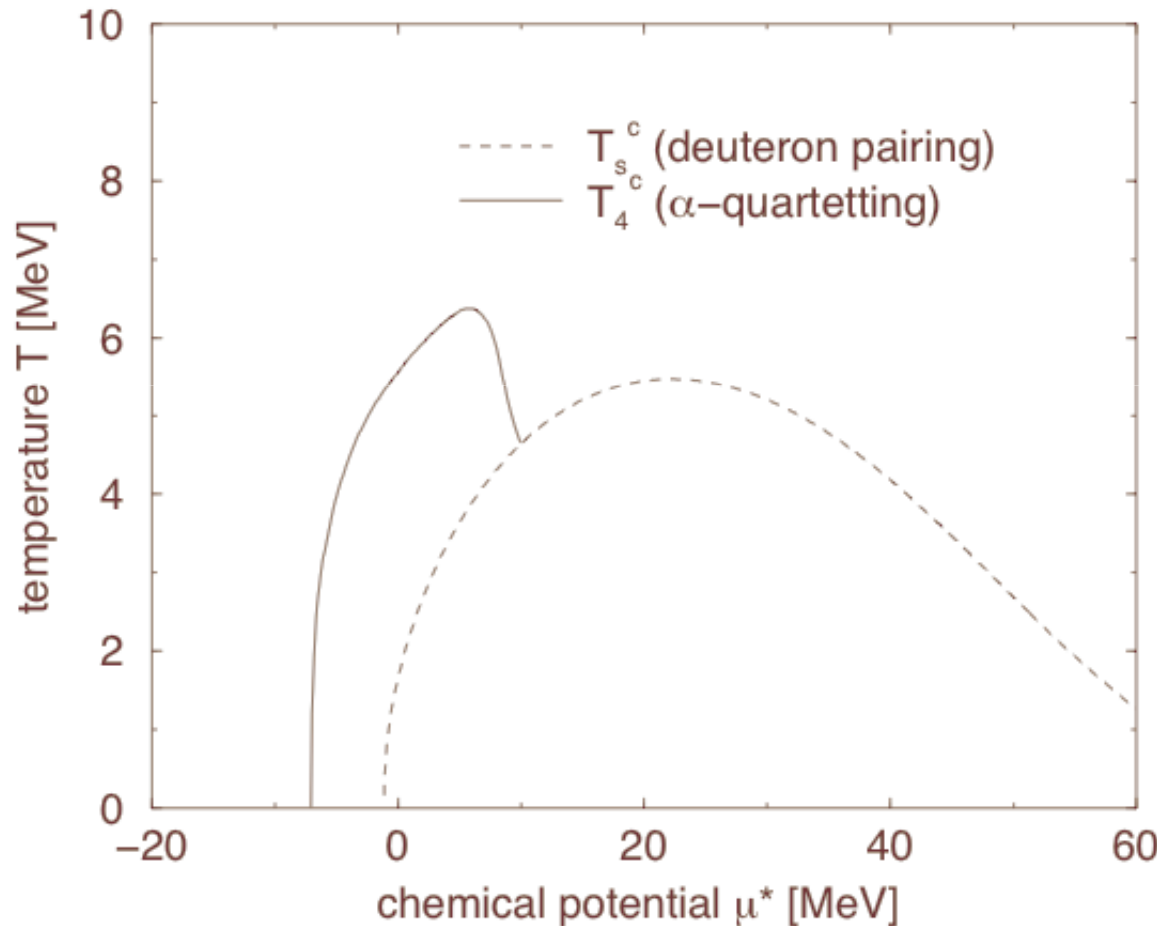


α -cluster-condensation (quartetting)

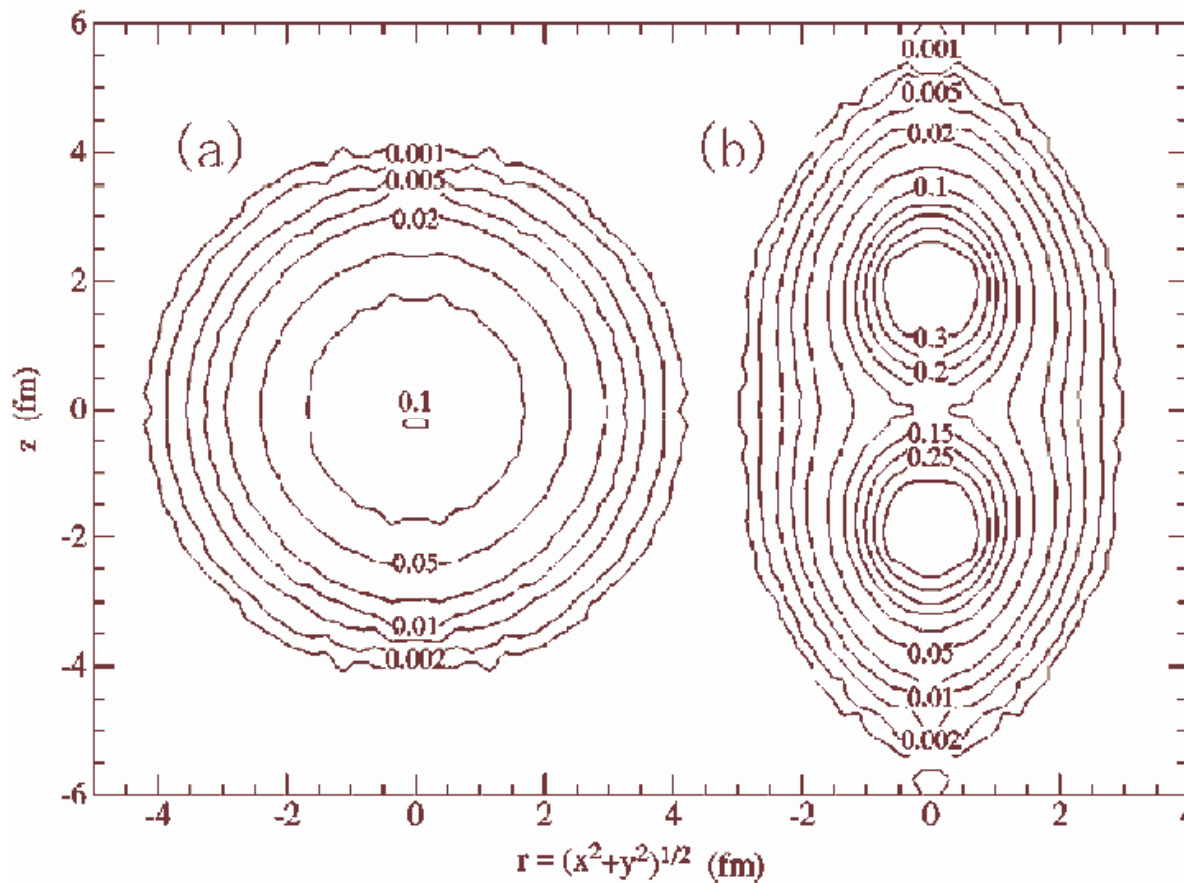


G. Röpke, A. Schnell, P. Schuck, and P. Nozieres, PRL 80, 3177 (98)

α -cluster-condensation (quartetting)



Alpha cluster structure of Be 8



R.B. Wiringa et al.,
PRC 63, 034605 (01)

Contours of constant density, plotted in cylindrical coordinates, for $8\text{Be}(0^+)$.
The left side is in the laboratory frame while the right side is in the intrinsic frame.

Self-conjugate 4n nuclei

^{12}C :

0^+ state at 0.39 MeV above the 3α threshold energy:
 α cluster interact predominantly in relative S waves,
gaslike structure

α -particle condensation in low-density nuclear matter
($\rho \leq \rho_0/5$)

$n\alpha$ cluster condensed states

– a general feature in $N = Z$ nuclei?

Self-conjugate 4n nuclei

$n\alpha$ nuclei: ^8Be , ^{12}C , ^{16}O , ^{20}Ne , ^{24}Mg , ...

Single-particle shell model, or

Cluster type structures

ground state, excited states

$n\alpha$ break up at the threshold energy $E_{n\alpha}^{\text{thr}} = nE_\alpha$

Variational ansatz

$$|\Phi_{n\alpha}\rangle = (C_\alpha^\dagger)^n |\text{vac}\rangle$$

α - particle creation operator

$$\begin{aligned} C_\alpha^\dagger &= \int d^3R e^{-\vec{R}^2/R_0^2} \\ &\times \int d^3r_1 \dots d^3r_4 \phi_{0s}(\vec{r}_1 - \vec{R}) a_{\sigma_1 \tau_1}^\dagger(\vec{r}_1) \dots \phi_{0s}(\vec{r}_4 - \vec{R}) a_{\sigma_4 \tau_4}^\dagger(\vec{r}_4) \end{aligned}$$

with

$$\phi_{0s}(\vec{r}) = \frac{1}{(\pi b^2)^{3/4}} e^{-\vec{r}^2/(2b^2)}$$

Variational ansatz

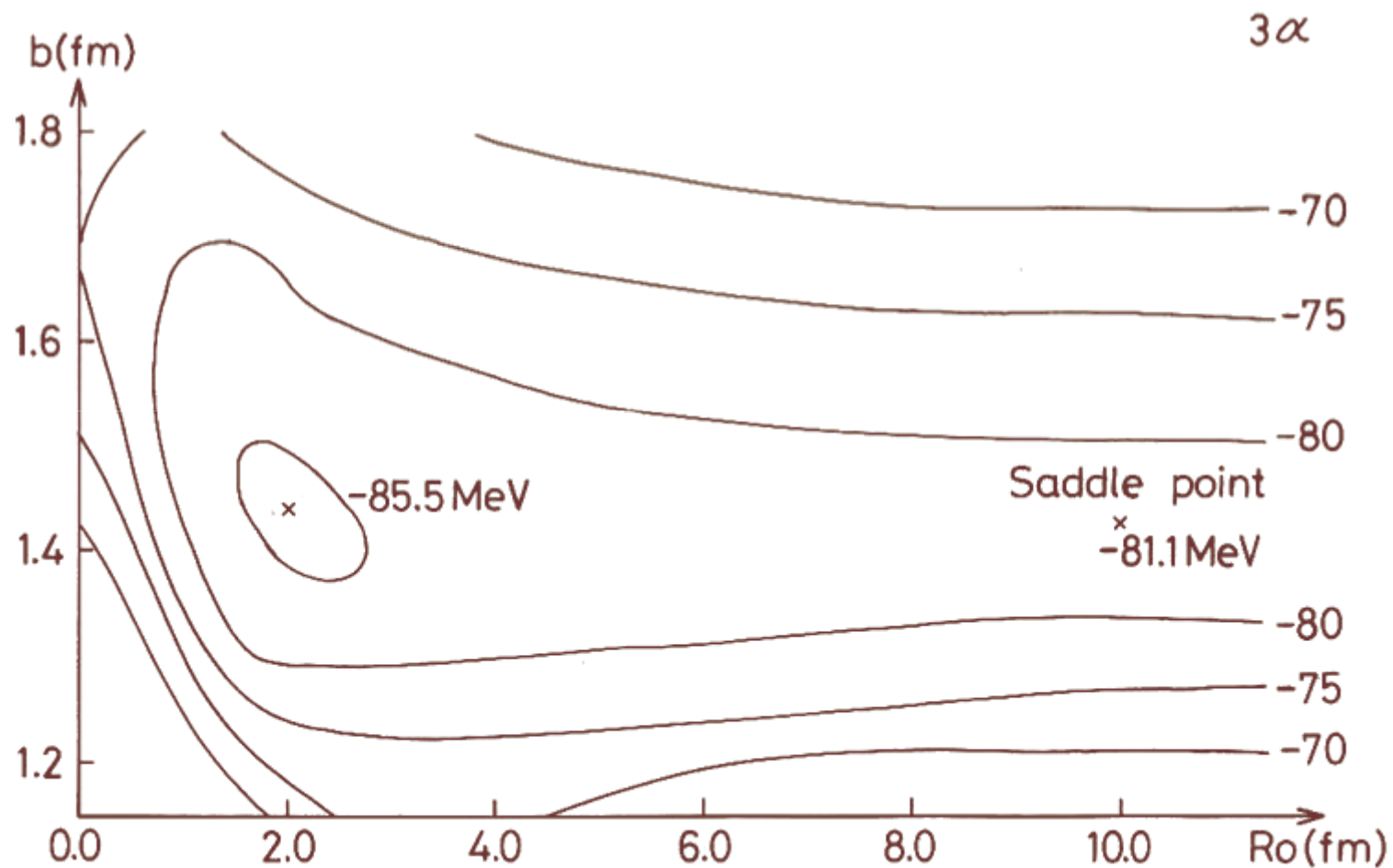
total $n\alpha$ wave function

$$\langle \vec{r}_1 \sigma_1 \tau_1 \dots \vec{r}_{4n} \sigma_{4n} \tau_{4n} | \Phi_{n\alpha} \rangle \\ \propto \mathcal{A} \left\{ e^{-\frac{2}{B^2} (\vec{X}_1^2 + \dots + \vec{X}_n^2)} \phi(\alpha_1) \dots \phi(\alpha_n) \right\}$$

where $B^2 = (b^2 + 2R_0^2)$, $\vec{X}_i = \frac{1}{4} \sum_n \vec{r}_{in}$,
 $\phi(\alpha_i) = e^{-\frac{1}{8b^2} \sum_{m>n}^4 (\vec{r}_{im} - \vec{r}_{in})^2}$ - internal α wave function

A. Tohsaki, H. Horiuchi, P. Schuck, G. Röpke, PRL **87**, 192501 (2001)

3 alpha variational energy



Results

		E_k (MeV)	E_{exp} (MeV)	$E_k - E_{n\alpha}^{\text{thr}}$ (MeV)	$(E - E_{n\alpha}^{\text{thr}})_{\text{exp}}$ (MeV)	$\sqrt{\langle r^2 \rangle}$ (fm)	$\sqrt{\langle r^2 \rangle}_{\text{exp}}$ (fm)
^{12}C	$k = 1$	-85.9	-92.16 (0_1^+)	-3.4	-7.27	2.97	2.65
	$k = 2$	-82.0	-84.51 (0_2^+)	+0.5	0.38	4.29	
	$E_{3\alpha}^{\text{thr}}$	-82.5	-84.89				
^{16}O	$k = 1$	-124.8 (-128.0)*	-127.62 (0_1^+) (-18.0)*	-14.8	-14.44	2.59	2.73
	$k = 2$	-116.0	-116.36 (0_3^+)	-6.0	-3.18	3.16	
	$k = 3$	-110.7	-113.62 (0_5^+)	-0.7	-0.44	3.97	
	$E_{4\alpha}^{\text{thr}}$	-110.0	-113.18				
	^{8}Be			-0.17	+0.1		

Tabelle 1: Comparison of the generator coordinate method calculations with experimental values. $E_{n\alpha}^{\text{thr}} = nE_\alpha$ denotes the threshold energy for the decay into α -clusters, the values marked by * correspond to a refined mesh.

Estimation of condensate fraction in zero temperature α -matter

$$n_0 = \frac{\langle \Psi | a_0^\dagger a_0 | \Psi \rangle}{\langle \Psi | \Psi \rangle}$$

destruction of the BEC of the ideal Bose gas:
thermal excitation, but also correlations

“excluded” volume for α -particles ≈ 20 fm 3 Singwi, 1958
at nucleon density $\rho = 0.048$ fm $^{-3}$ filling factor $\approx 28\%$
(liquid ${}^4\text{He}$: 8 % condensate),
destruction of the condensate at $\approx \rho_0/3$

Estimation of condensate fraction in zero temperature α -matter

α -cluster condensate in ^{12}C , ^{16}O :
resonating group method
occupation numbers of α -orbits in ^{12}C

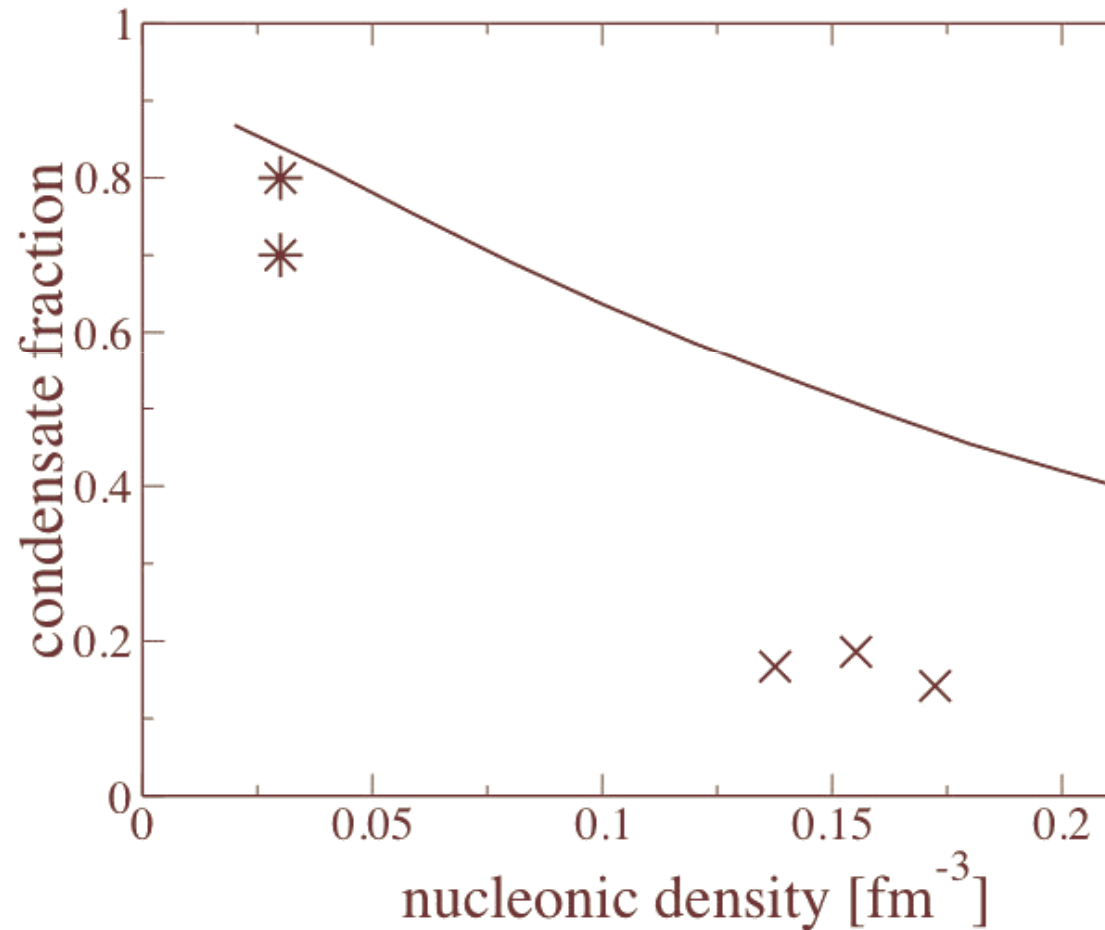
	RMS radii	S-orbit	D-orbit	G-orbit
O_1^+ (g.s.)	2.44 fm	1.07	1.07	0.82
O_2^+	4.31 fm	2.38	0.29	0.16

80 % condensate at 1/8 nuclear matter density

T. Yamada, P. Schuck : $(2.16 - \text{normal})/3 \approx 60\%$

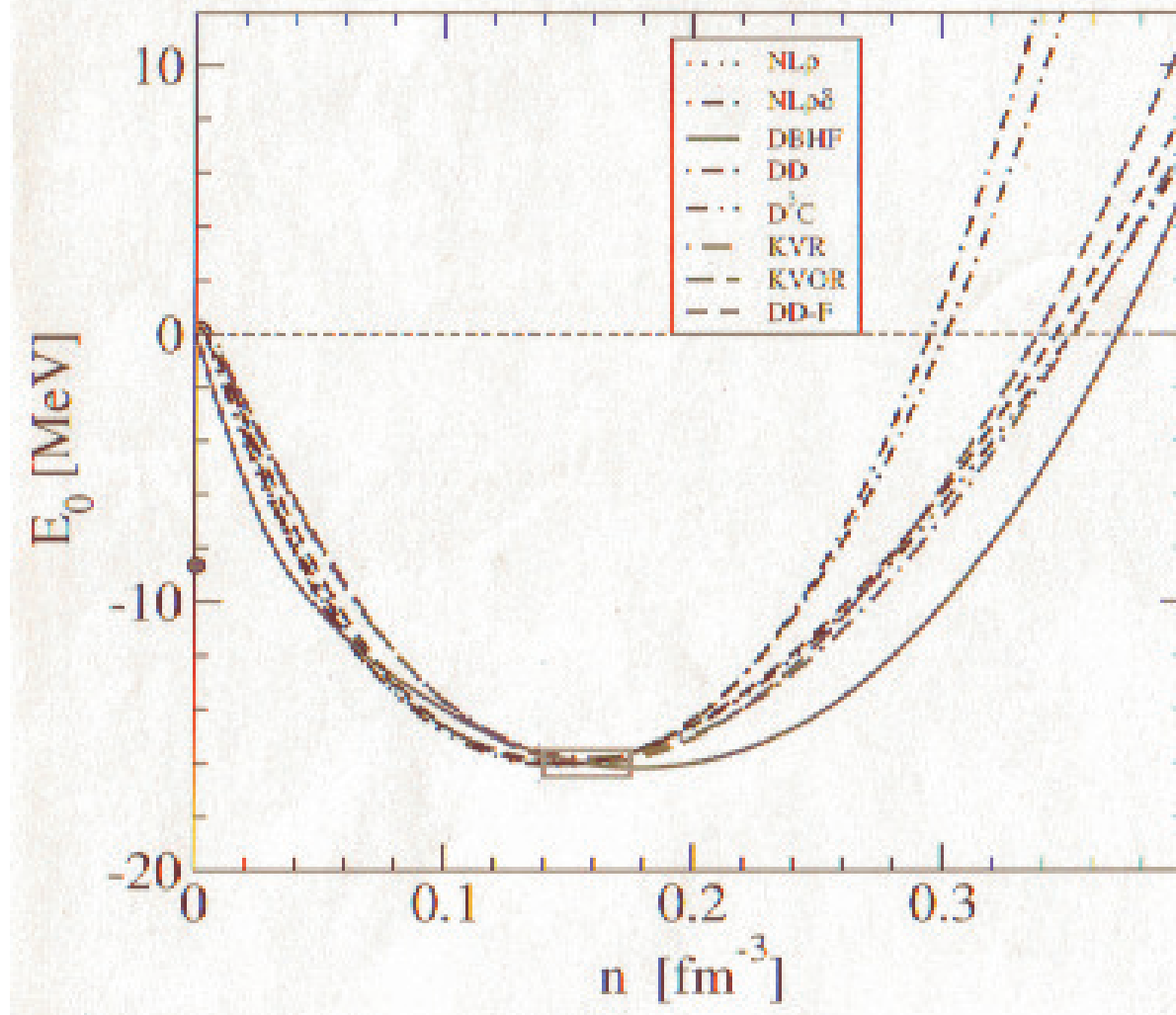
Suppresion of condensate fraction

- Alpha-alpha interaction (Ali/Bodmer), no Pauli blocking:
- Variational calculation (Clark/Jastrow approach to the alpha-particle condensate amplitude) (crosses)
- First order approximation (full line)
- Yamada/Schuck's result for condensate in C12 - O2+ (stars)



Quasiparticle approximation for nuclear matter

Equation of state for symmetric matter



Summary

- The low-density limit of the nuclear matter EoS can be rigorously treated.
The Beth-Uhlenbeck virial expansion is a benchmark.
- An extended quasiparticle approach can be given for single nucleon states and nuclei. In a first approximation, self- energy and Pauli blocking is included. An interpolation between low and high densities is possible.
- Compared with the standard quasiparticle approach, significant changes arise in the low-density limit due to clustering. Examples are Bose-Einstein condensation (quartetting), and the behavior of the symmetry energy.

Thanks

to D. Blaschke, C. Fuchs, J. Natowitz, T. Klaehn,
S. Shlomo, P. Schuck,
A. Sedrakian, K. Sumiyoshi, S. Typel, H. Wolter
for collaboration

to you
for attention

Correlations in the medium

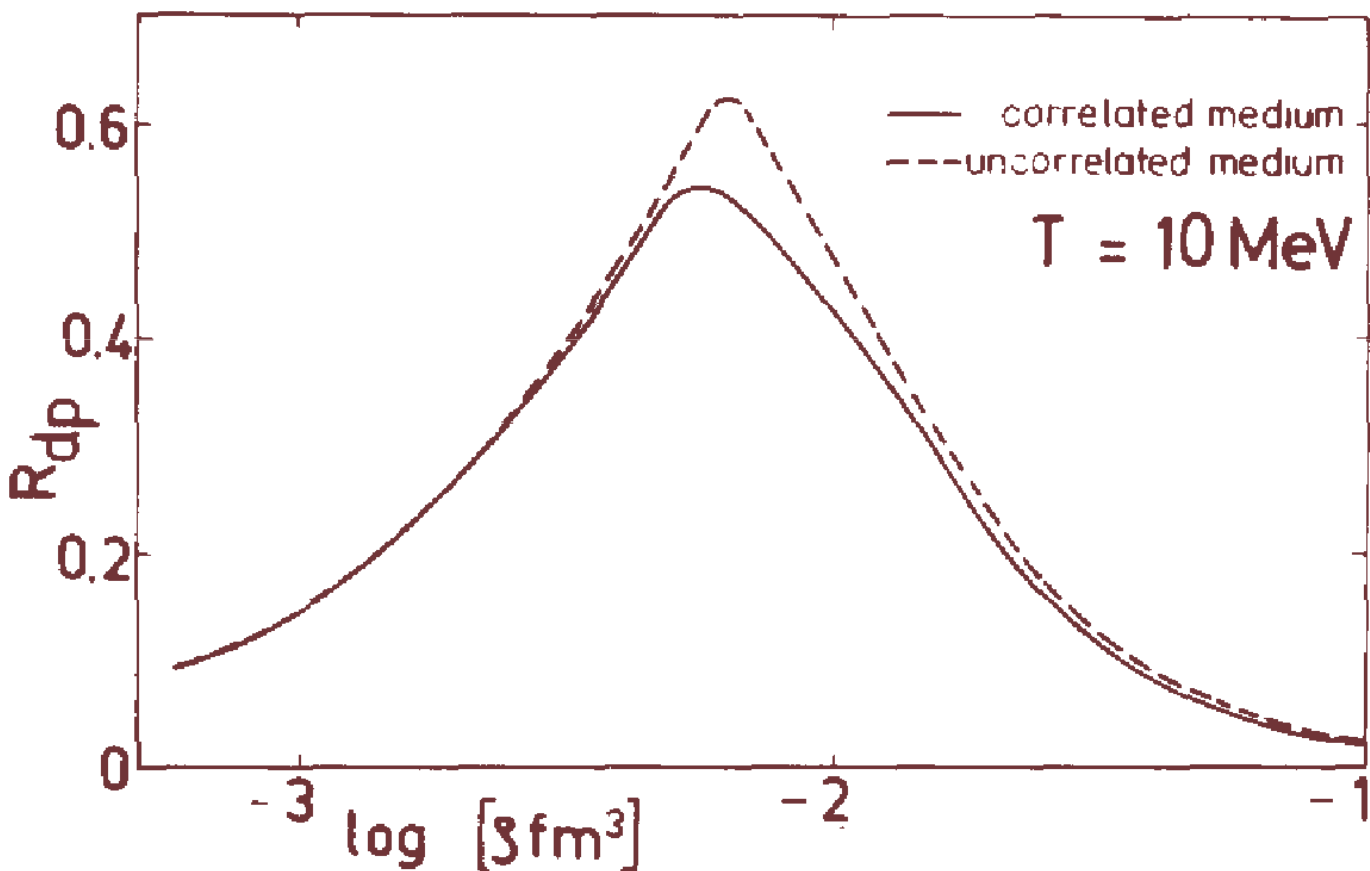
$$\Sigma_2 =$$

The equation $\Sigma_2 =$ is followed by a sum of six diagrams, each consisting of a horizontal line with two external vertices labeled x , a vertical dashed line connecting them, and a loop above labeled $(2x)$. The diagrams differ in the internal structure of the loop:

- Diagram 1: A simple loop with one internal line.
- Diagram 2: A loop with two internal lines crossing.
- Diagram 3: A loop with three internal lines forming a triangle.
- Diagram 4: A loop with four internal lines forming a rectangle.
- Diagram 5: A loop with five internal lines forming a pentagon.
- Diagram 6: A loop with six internal lines forming a hexagon.

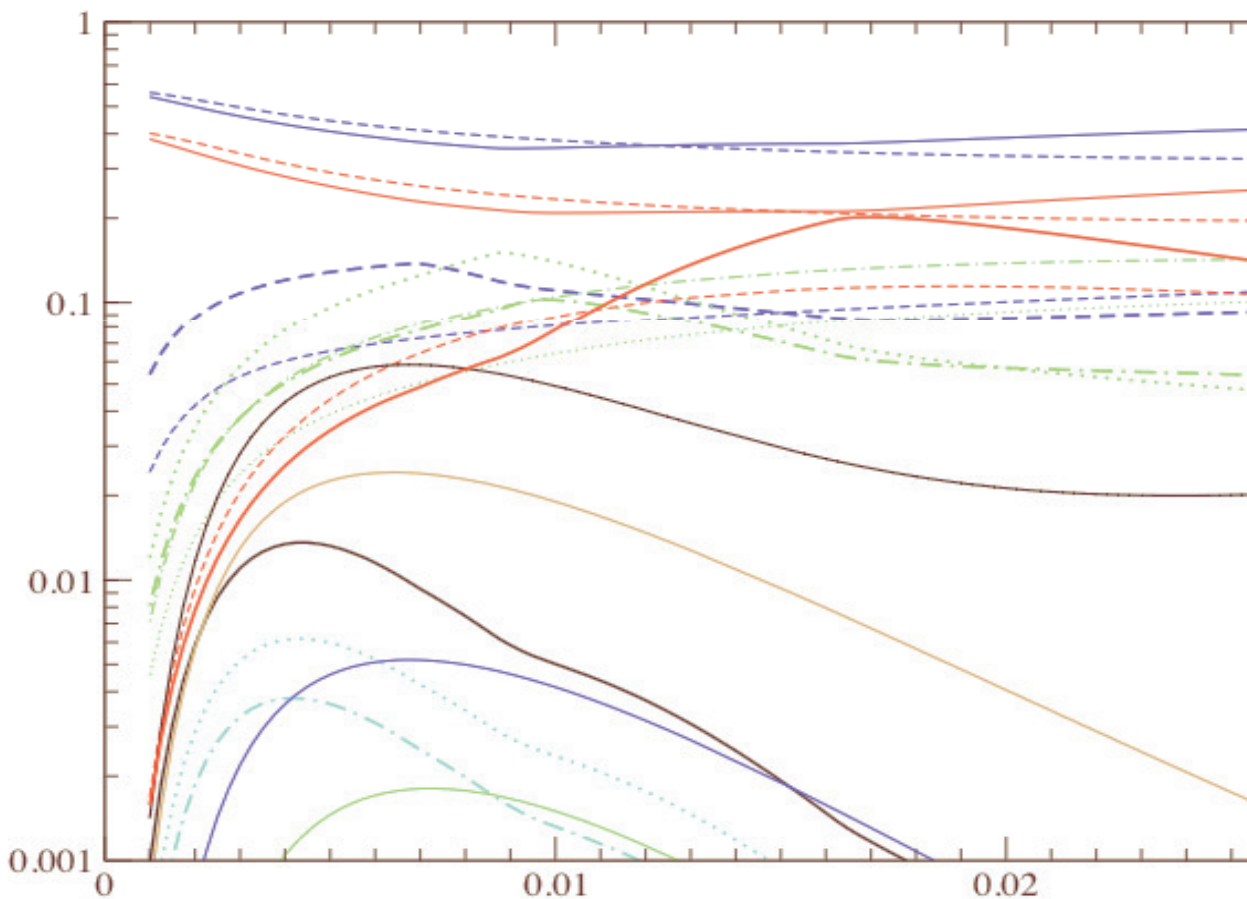
Plus signs are placed between the first three diagrams and between the last three diagrams.

Account of two-particle correlations in the medium



Heavy nuclei abundances in nuclear matter

T=10 MeV, asymmetry 0.42, as function of baryon density



n, p, d, t, He3, He4, Li5,....

Alpha-condensate (quartetting) in $4n$ symmetric nuclei

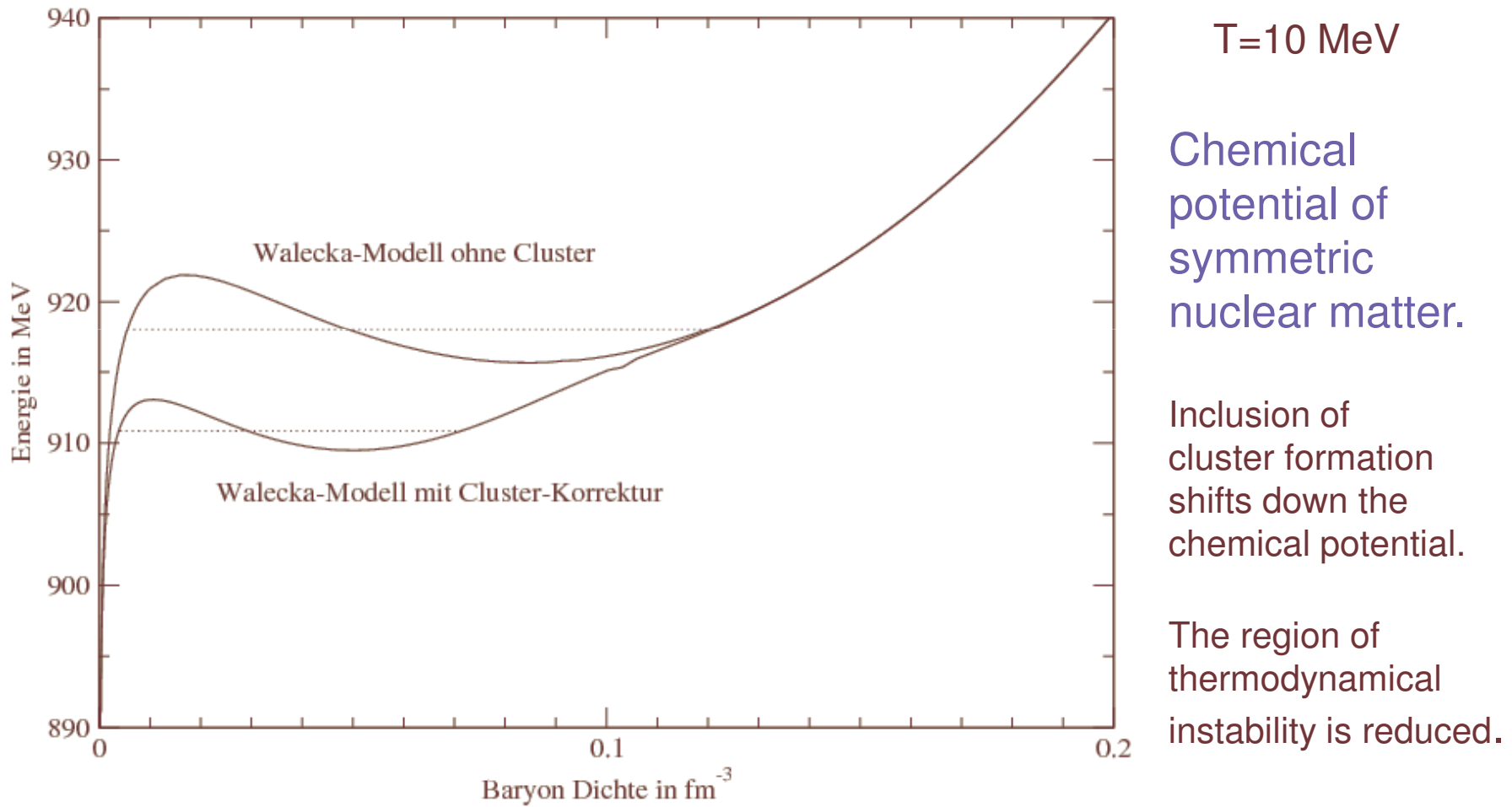
- A. Tohsaki, H. Horiuchi, P. Schuck, G. Röpke,
Phys. Rev. Lett. **87**, 192501 (2001).
- G. Röpke, A. Schnell, P. Schuck, and P. Nozieres,
Phys. Rev. Lett. **80**, 3177 (1998).
- Y. Funaki, A. Tohsaki, H. Horiuchi, P. Schuck, G. Röpke,
Phys. Rev. C **67**, 051306(R) (2003); Eur. Phys. J. A **28**, 259 (2006).
- T. Yamada, P. Schuck,
Phys. Rev. C **69**, 024309 (2004).

Approximations to the symmetry energy

QuickTime™ and a
TIFF (LZW) decompressor
are needed to see this picture.

S. Kubis,
Neutron stars with
non-homogeneous
core,
Talk 26.2.08, Ladek

Influence of cluster formation on the equation of state



G.R., A. Grigo (2003)